

1 **Short Title:** Genetic Architecture of Gene Expression in Tomato

2

3 **Corresponding author:**

4 Neelima R. Sinha

5 Department of Plant Biology

6 1002 Life Sciences

7 One Shields Ave.

8 Phone: (530) 754-8441

9 Fax: (530) 752-5410

10 e-mail: nrsinha@ucdavis.edu

11

12 **Research area:** Genes, Development and Evolution

13

14

15

16

17

18

19

20

21

22

23

24

25

26 **Title: eQTL in a Precisely Defined Tomato Introgression Population Reveal**
27 **Genetic Regulation of Gene Expression Patterns Related to Physiological**
28 **and Developmental Pathways**

29

30 Aashish Ranjan^{#a¶}, Jessica M. Budke[¶], Steven D. Rowland[¶], Daniel H.
31 Chitwood^{#b}, Ravi Kumar^{#c}, Leonela Carriedo, Yasunori Ichihashi^{#d}, Kristina
32 Zumstein, Julin N. Maloof, and Neelima R. Sinha

33 Department of Plant Biology, University of California at Davis, Davis, California,
34 United States of America

35

36 [¶]These authors contributed equally to this work.

37

38 **Summary:** Genetical genomics approach in tomato identified genetic hotspots
39 that regulate gene expression patterns relating to diverse biological processes
40 such as plant development, photosynthesis and defense.

41

42

43

44

45

46 **Footnotes:**

47 **Funding information:** This work is supported through a National Science
48 Foundation grant (IOS-0820854) awarded to NRS and JNM. DHC was a fellow of
49 the Life Sciences Research Foundation funded through the Gordon and Betty
50 Moore Foundation. JMB is a recipient of Katherine Esau Postdoctoral Fellowship
51 at UC Davis.

52 **Present Address:**

53 ^{#a} : National Institute of Plant Genome Research, New Delhi, India.

54 ^{#b} : Donald Danforth Plant Science Center, St. Louis, Missouri, United States of
55 America.

56 ^{#c} : Novozymes, Davis, California, United States of America.

57 ^{#d} : RIKEN Center for Sustainable Resource Science, Yokohama, Kanagawa,
58 Japan.

59

60 **Corresponding author email:** nrsinha@ucdavis.edu

61

62

63

64

65 **Abstract**

66 Variation in gene expression, in addition to sequence polymorphisms, is known
67 to influence developmental, physiological and metabolic traits in plants. Genetical
68 genomics approaches on genetic mapping populations have facilitated the
69 identification of expression Quantitative Trait Loci (eQTL), the genetic
70 determinants of variation in gene expression patterns. We used an introgression
71 population developed from the wild desert-adapted *Solanum pennellii* and
72 domesticated tomato *Solanum lycopersicum* to identify the genetic basis of
73 transcript level variation. We established the effect of each introgression on the
74 transcriptome through differential gene expression analysis, and identified ~7,200
75 eQTL regulating the expression of 5,300 genes. Barnes-Hut *t*-distributed
76 stochastic neighbor embedding clustering identified 42 modules revealing novel
77 associations between gene expression patterns and biological processes. The
78 results showed a complex genetic architecture of global gene expression pattern
79 in tomato. Several genetic hotspots regulating a large number of gene
80 expression patterns relating to diverse biological processes such as plant
81 defense and photosynthesis were identified. We identified important eQTL
82 regulating gene expression patterns related to leaf number and complexity, and
83 hypocotyl length. Genes associated with leaf development showed an inverse
84 correlation with photosynthetic gene expression but their regulation was
85 dispersed across the genome. This is the first comprehensive insight into the
86 global regulation of transcript abundance in tomato and its influence on plant

87 phenotypes, which sets the stage for identifying gene/s underlying these
88 regulatory loci.

89

90 **Introduction**

91 The genetic basis of many qualitative and quantitative phenotypic
92 differences in plants has been associated with sequence polymorphisms and the
93 corresponding changes in gene function. However, differences in the levels of
94 gene expression, without underlying changes in coding sequences, also
95 significantly influence plant phenotypes. Closely related plant species often have
96 little coding sequence divergence, nonetheless they often develop unique
97 physiological, metabolic, and developmental characteristics indicating that
98 patterns of gene expression are important in species-level phenotypic variation
99 (Kliebenstein, 2009; Koenig et al., 2013). Phenotypic differences attributed to
100 variations in gene expression patterns have been found to influence disease
101 resistance, insect resistance, phosphate sensing, flowering time, circadian
102 rhythm, and plant development (Kroymann et al., 2003; Werner et al., 2005;
103 Clark et al., 2006; Zhang et al., 2006; Svistoonoff et al., 2007; Chen et al., 2010;
104 Hammond et al., 2011).

105 Global gene expression changes across defined genetic backgrounds
106 have been used to identify expression Quantitative Trait Loci (eQTL) through
107 genetical genomics approaches (Jansen and Nap, 2001; Kliebenstein, 2009;
108 Druka et al., 2010; Chitwood and Sinha, 2013). An eQTL is a chromosomal

109 region that drives variation in gene expression patterns (i.e., transcript
110 abundance) between individuals of a genetic mapping population and can be
111 treated as a heritable quantitative trait (Brem et al., 2002; Kliebenstein, 2009;
112 Cubillos et al., 2012). Recent advances in next-generation sequencing have
113 enabled high-throughput genotyping and transcript abundance estimation to
114 provide direct readouts of the regulatory changes in mapping populations,
115 allowing identification of thousands of eQTL in a single experiment (Pickrell et al.,
116 2010; Chitwood and Sinha, 2013; Battle et al., 2015). Global eQTL studies in
117 animals, fungi, and plants have provided genetic insights into the transcriptional
118 regulation of these organisms (Brem and Kruglyak, 2005; Keurentjes et al., 2007;
119 West et al., 2007; Schadt et al., 2008; Hammond et al., 2011; Holloway et al.,
120 2011; Zhang et al., 2011; Cubillos et al., 2012).

121 Depending upon the proximity to the gene being regulated, eQTL can be
122 classified into two groups: *cis*-eQTL when the physical location of an eQTL
123 coincides with the location of the regulated gene, and *trans*-eQTL when an eQTL
124 is located at a different position from the gene being regulated (Kliebenstein,
125 2009). eQTL studies with the model plant *Arabidopsis* underlined the significance
126 and contributions of *cis*- and *trans*-eQTL (DeCook et al., 2006; West et al., 2007;
127 Holloway and Li, 2010). *Cis*-eQTL have a significant effect on local expression
128 levels, whereas *trans*-eQTL often have global influences on gene regulation.
129 Individual genes can have multiple *trans*-eQTL contributing to the regulation of
130 their expression pattern. Identification of *trans*-acting eQTL hotspots, defined as
131 regions affecting the expression of a significantly larger number of genes than

132 expected, have been found in many eQTL studies. Genes underlying an eQTL
133 hotspot could be master transcription factors controlling the expression of a suite
134 of genes that act in the same biological process or pathway. For example, eQTL
135 hotspots in *Arabidopsis* co-locate with the *ERECTA* locus, which has been
136 shown to pleiotropically influence many traits including those regulating
137 morphology (Keurentjes et al., 2007). In addition, the eQTL identified using
138 pathogen challenged tissues in barley were enriched for genes related to
139 pathogen response (Chen et al., 2010; Druka et al., 2010). Similarly the rice *sub1*
140 locus, which regulates submergence tolerance, controls the activity of an
141 ethylene response factor with significant *trans* effects (Fukao et al., 2006; Xu et
142 al., 2006). Thus eQTL analyses have the potential to reveal a genome-wide view
143 of the complex genetic architecture of gene expression regulation, the underlying
144 gene regulatory networks, and may also identify master transcriptional regulators.

145 Cultivated tomatoes, along with their wild-relatives, harbor broad genetic
146 diversity and large phenotypic variability (Moyle, 2008; Ranjan et al., 2012).
147 Wide interspecific crosses bring together divergent genomes and hybridization of
148 such diverse genotypes leads to extensive gene expression alterations
149 compared to either parent. Gene expression in hybrids often deviates from purely
150 additive effects and may contribute to hybrid vigor and in nature can act as a
151 source of variation for selection to act upon (Hegarty et al., 2008). Introgression
152 lines (ILs), developed by crosses between wild-relatives and the cultivated
153 tomato to bring discrete wild-relative genomic segments into the cultivated
154 background, have proved to be a useful genetic resource for genomics and

155 molecular breeding studies. One such highly characterized introgression
156 population was developed from the wild desert-adapted species *Solanum*
157 *pennellii* and domesticated *Solanum lycopersicum* cv. M82 (Eshed and Zamir,
158 1995; Liu and Zamir, 1999). These two species exhibit large phenotypic
159 differences for both developmental and metabolic traits. This IL population has
160 been successfully used to map numerous QTL for metabolites, enzymatic activity,
161 yield, fitness traits, and developmental features, such as leaf shape, size, and
162 complexity (Frary et al., 2000; Holtan and Hake, 2003; Fridman et al., 2004;
163 Chitwood et al., 2013; Muir et al., 2014). Though these studies led to fine
164 mapping of candidate genes underlying identified QTL, phenotypic QTL mapping
165 does not provide insight into the molecular regulation and gene networks
166 underlying a trait. Comparative transcriptomics using cultivated and wild species
167 enables identification of transcript abundance variation potentially underlying trait
168 differences, such as salt tolerance, between species (Koenig et al., 2013).
169 However, the genetic regulators of these transcriptional differences between the
170 species still need to be elucidated. Therefore, we used a genetical genomics
171 approach to identify the genetic basis of transcript level variation in tomato using
172 the *S. pennellii* introgression lines.

173 Using both genomic DNA and RNAseq reads we recently pinpointed the
174 exact gene content harbored in the introgression regions for the *S. pennellii* ILs
175 and identified more than a thousand QTL underlying plant developmental traits,
176 including leaf traits (Chitwood et al., 2013). Here we report on a comprehensive
177 transcriptome profile of the ILs, a comparison between the gene expression

178 patterns of the ILs and the cultivated M82 background (differential gene
179 expression – DE), as well as a global eQTL analysis to identify patterns of
180 genetic regulation of transcript abundance in the tomato shoot apex. We have
181 identified more than 7,200 *cis*- and *trans*-eQTL in total, which regulate the
182 expression patterns of 5,300 genes in tomato. Additional analyses using Barnes-
183 Hut *t*-distributed stochastic neighbor embedding (BH-SNE) (van der Maaten,
184 2013) identified 42 modules revealing novel associations between gene
185 expression patterns and biological processes. The gene expression patterns
186 under strong genetic regulation are related to plant defense, photosynthesis, and
187 plant developmental traits. We also report important eQTL regulating gene
188 expression pattern associated with leaf number, complexity, and hypocotyl length
189 phenotypes.

190

191 **Results and Discussion**

192 **Transcriptome Profiling of Introgression Lines**

193 RNAseq reads obtained from the tomato shoot apex with developing
194 leaves and hypocotyl were used to identify differentially expressed (DE) genes
195 between each *S. pennellii* IL and the cultivated M82 (Supplemental Dataset 1).
196 The total number of genes differentially expressed for each IL both in *cis* (in this
197 population reflecting “local” level regulation either from within a gene itself or
198 other genes in the introgression) and *trans*, along with the number of genes in
199 the introgression regions, are presented in Figure 1 and Supplemental Table I.
200 There was a strong correlation between the number of genes in the introgression

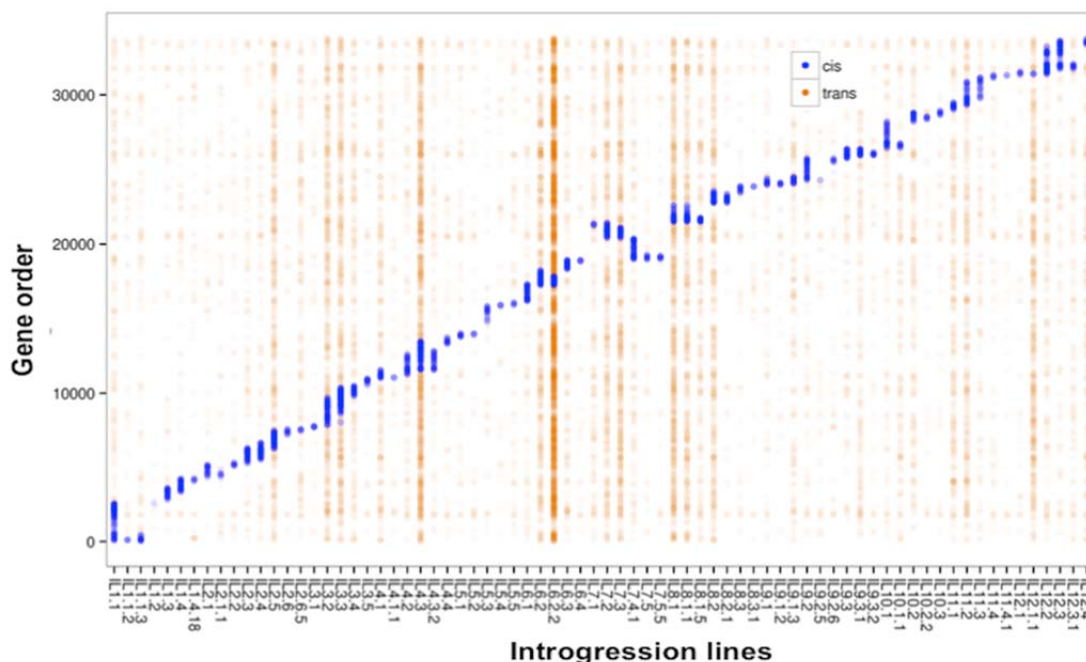


Figure 1. Transcriptome profile of the tomato introgression lines. Differentially expressed genes for the ILs compared to cultivated parent M82. Y-axis shows all the tomato genes starting from the first gene on chromosome 1 to the last gene on chromosome 12, and X-axis depicts the individual ILs. Genes differentially expressed within the introgression regions (in *cis*) are shown as blue points and differentially expressed genes in *trans* (outside) the introgression region are shown as orange points.

201 regions and the number of DE genes in *cis* (Supplemental Figure S1A). In
202 contrast, the number of DE genes in *trans* was poorly correlated with
203 introgression size (Supplemental Figure S1B). ILs showing higher total number of
204 DE genes, such as IL6.2.2 and IL4.3, showed regulation of most of the DE genes
205 in *trans* (Figure 1, Supplemental Table I, Supplemental Figure S2). IL12.1.1,
206 despite having one of the smallest introgressions, showed 96% of ~500 DE
207 genes regulated in *trans* (Supplemental Table I, Supplemental Figure S2). In
208 contrast, IL1.1 and IL12.3, the ILs with highest number of genes in the
209 introgression regions, showed smaller numbers of total and *trans* DE genes
210 (Figure 1, Supplemental Table I, Supplemental Figure S2). Together these
211 examples suggest that specific loci and not the introgression size determine gene
212 regulation in *trans*. For example, *S. pennellii* chromosomal regions introgressed

213 in IL6.2.2 and IL12.1.1 have stronger genetic influence on global transcript
214 abundance than the regions introgressed in IL1.1 and IL2.3. This could, in part,
215 be due to the presence of genes encoding key transcription factors or
216 developmental regulators in these regions with strong influence on gene
217 expression pattern as is seen in the *ERECTA* containing genomic region in
218 Arabidopsis (Keurentjes et al., 2007). A total of 7,943 unique tomato genes were
219 DE between the ILs and cv. M82, representing approximately one third of the
220 ~21,000 genes with sufficient sequencing depth to allow DE analysis. This
221 suggests that in addition to protein coding differences, transcriptional regulation
222 of less than one third of all genes accounts for most of the phenotypic and trait
223 differences between the ILs and the cultivated parent. Among the 7,943 DE
224 genes, 2790 (35%) genes were under *cis*-regulation only, 3603 (45%) genes
225 were under *trans*-regulation only, and 1550 (20%) genes were under both *cis*-
226 and *trans*- regulation. Of these DE genes 4057 (51%) were DE in only one IL,
227 840 genes were DE in 5 or more ILs, 8 genes were DE in over 50 ILs, and a
228 single gene was DE in 70 ILs (Supplemental Dataset 2, Supplemental Figure
229 S3A). The genetic regulation of many transcripts by more than one introgression
230 and in *trans* suggests a complex genetic architecture of global transcript
231 regulation in tomato, a phenomenon noticed in many other eukaryotes such as
232 Arabidopsis, yeast, mice, and humans (Brem and Kruglyak, 2005; West et al.,
233 2007; Schadt et al., 2008).

234

235 **Global eQTL analysis at IL-bin level**

236 Identifying eQTL localized to subsets of the introgressions, based on overlaps
237 between them, enabled us to narrow down the regions that contain the regulatory
238 loci. This analysis brings us one step closer to identifying potential candidates
239 that influence gene expression patterns in tomato. The 20,795 genes with
240 sufficient read depth in the RNAseq libraries were analyzed across 74 ILs with
241 112 bins defined based on the overlap of introgression regions from *S. pennellii*
242 in the cv. M82 background (Chitwood et al., 2013) (Supplemental Figure S4). We
243 found 7,225 significant eQTL involving 5,289 unique genes across the 74 ILs
244 (Figure 2; Supplemental Dataset 3). These 7,225 significant eQTL (located in
245 bins) were assigned the following designations (Supplemental Figure S4): *cis*
246 (defined as local gene regulation within the same bin) - if the gene was located
247 on the bin it is correlated with, *trans* (distant) - if the gene was correlated with a
248 bin that is neither the bin it is on nor a bin that shares an overlapping IL with the
249 correlated bin, and *chrom0* - if the gene is not located on any of the
250 chromosomes and thus lies in the unassembled part of the genome. When a
251 gene has a designation *cis*-eQTL and a secondary correlation was found with a
252 bin that shares an overlapping introgression this secondary correlation was not
253 designated as an eQTL (Supplemental Figure S4). When a gene does not have a
254 designated *cis*-eQTL and a correlation was found with a bin that shares an
255 overlapping introgression this correlation was designated as a *trans*-eQTL
256 (Supplemental Figure S4). This resulted in a total of 1,759 *cis*-up and 1,747 *cis*-
257 down eQTL, 2,710 *trans*-up and 920 *trans*-down eQTL, and 51 *chrom0*-up and
258 38 *chrom0*-down eQTL (Spearman's rho values, Supplemental Figure S5,

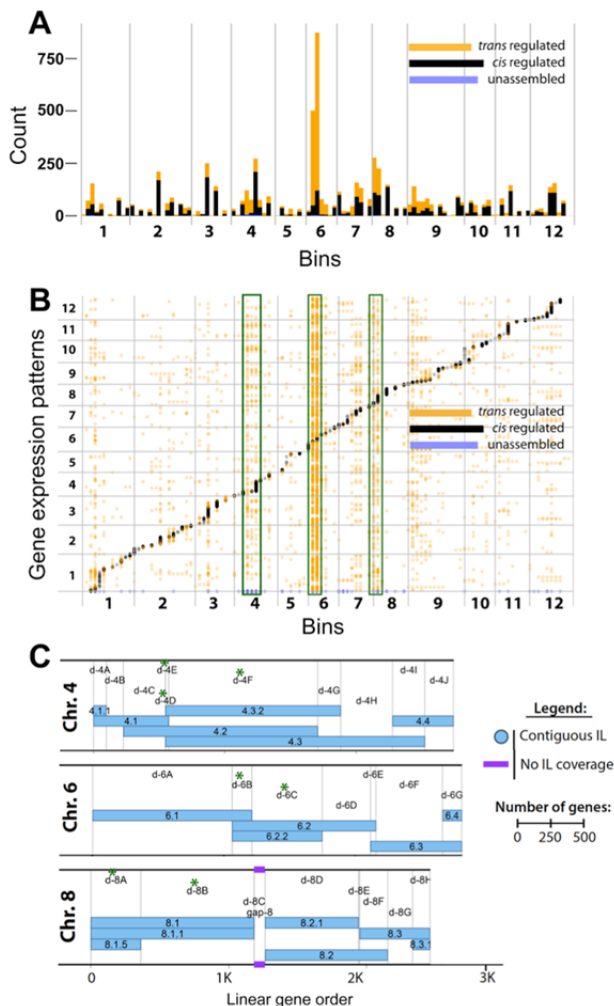


Figure 2. Cis- and Trans-eQTL plotted by bin across the 12 chromosomes of *S. lycopersicum* cv. M82. A) Stacked bar graph showing the sum of the number of eQTL mapping to each bin. B) Dotplot showing each eQTL arranged vertically by bin and horizontally by the location of the gene expression pattern it regulates. Bins with the largest numbers of *trans*-eQTL (4D, 4E, 4F, 6B, 6C, 8A, 8B) are highlighted by green boxes. C) Map of chromosomes 4, 6, and 8 showing the overlapping IL regions, which define the bins (Modified from Chitwood et al., 2013). Bins with the largest numbers of *trans*-eQTL are indicated by green asterisks.

259 Supplemental Table II). The majority of genes (over 4,000 out of 5,289) are
 260 under the regulation of a single eQTL (3,134 *cis*-, 1,014 *trans*-, and 19 *chromo0*-;
 261 Supplemental Figure S3B). This shows the predominance of *cis*-eQTL for genetic
 262 regulation of transcript expression patterns in the tomato ILs. Similar correlation
 263 between transcript-level variation and genome-wide sequence divergence within
 264 seven Arabidopsis accessions was reported to be due to *cis* control of a majority
 265 of the detected variation (Kliebenstein et al., 2006).

266 Several bins harbor a large number and/or large proportion of significant
267 eQTL (Supplemental Dataset 4). The bins with over 100 significant *trans*-eQTL
268 are on chromosomes 6, 8, and 4 (respectively 6C = 753, 6B = 452, 8A = 169, 8B
269 = 128, 4D = 117). The number of genes in each bin is highly variable ranging
270 from 1 to over 1890. Thus another metric to assess the influence of a particular
271 bin is the number of significant *trans*-eQTL divided by total number of genes per
272 bin. Bins with over 1.5 significant *trans*-eQTL per gene include 4D (117.0), 7D
273 (14.7), 8C (8.0), 6B (3.0), 4E (2.5), and 3B (1.8). As expected, bins containing
274 over 100 significant *cis*-eQTLs are scattered across the genome (Supplemental
275 Dataset 4). Three bins, 1F, 3I and 8G, that each contain over 100 genes, have
276 no significant *trans*- or *cis*-eQTL and are transcriptionally silent (Supplemental
277 Dataset 4). The abundance of *trans*-eQTL on chromosomes 4, 6, and 8
278 strengthens the idea that *trans*-eQTL are clustered in *trans*-eQTL hotspots, as
279 reported in other organisms, and these hotspots control the expression levels of
280 a large number of transcripts (Brem et al., 2002; Schadt et al., 2003). The
281 resolution in this analysis is at the level of bin, and these significant eQTL likely
282 map to a smaller number of genes within the bins. However functional
283 classification of genes being regulated by these eQTL and phenotypic
284 association with the relevant ILs provides important insights into the candidate
285 genes in the bin.

286

287 **Clustering eQTL targets into modules defined by expression patterns**

288 In order to functionally categorize the eQTL regulated genes, Barnes-Hut
289 *t*-distributed stochastic neighbor embedding (BH-SNE, van der Maaten, 2013)
290 was performed on the target genes to detect novel associations between gene
291 expression patterns. The 5,289 genes with significant eQTL were mapped using
292 BH-SNE (as explained in Materials and Methods) based on similarities in their
293 expression patterns across the ILs. The exaggerated separation of non-
294 neighboring clusters in this method improves 2D resolution, allowing identification
295 of novel groupings not readily apparent in other clustering methods. This resulted
296 in 42 distinct modules containing 3,592 genes (Figure 3). Seventeen of these
297 modules had significant GO enrichment (p-value <0.05) with each module
298 consisting of gene expression patterns either predominately regulated by *cis*- or
299 *trans*-eQTL (Supplemental Table III). To determine which ILs are important for
300 module regulation, the median expression value of module genes for each IL was
301 calculated and used to identify ILs with significantly altered module gene
302 expression.

303 Three modules were present in all mappings of the BH-SNE (van der
304 Maaten and Hinton, 2008) determined through iterations of DBscan analysis and
305 GO enrichment, and were designated as landmark modules (Figure 3B;
306 Supplemental Figure S6; Supplemental Dataset 5; Supplemental Table III). The
307 largest module had a GO enrichment for photosynthesis and related processes,
308 and significant *trans*-eQTL scattered widely across the genome with no bin or IL
309 identified as the primary regulating region (Figure 4B; Supplemental Figure S6A;
310 Supplemental Dataset 5 & 6). The second landmark module was enriched for

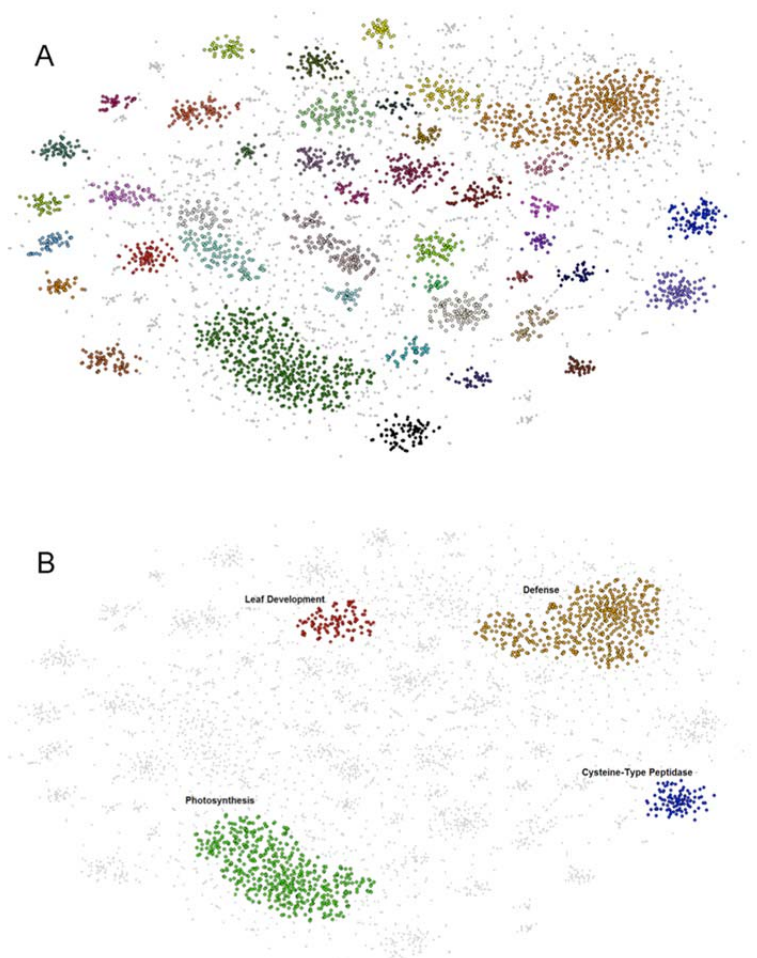


Figure 3. BH-SNE 2D mapping of eQTL. (A) Forty-two distinct modules identified by DBscan from the mapping generated by BH-SNE analysis. (B) The three modules defined as landmark modules: photosynthesis, defense and cysteine-type peptidase activity and the leaf development module's position within the mapping. Modules are false colored.

311 gene expression patterns with roles in defense, metabolism, and signaling with
312 the majority of their *trans*-eQTL mapped to IL6.2 and 6.2.2 (Figure 4A;
313 Supplemental Figure S6B; Supplemental Dataset 5 & 7). The third module, which
314 is enriched for gene expression patterns with cysteine-type peptidase activity,

315 was predominately composed of genes regulated by *cis*-eQTL on IL 4.2, 4.3, and
316 4.3.2 (Bins 4E & 4F) (Figure 4C; Supplemental Figure S6C; Supplemental
317 Dataset 5 & 8). A cluster of genes enriched for “peptidase regulation” also
318 emerged from a transcriptome study of leaf development for three tomato

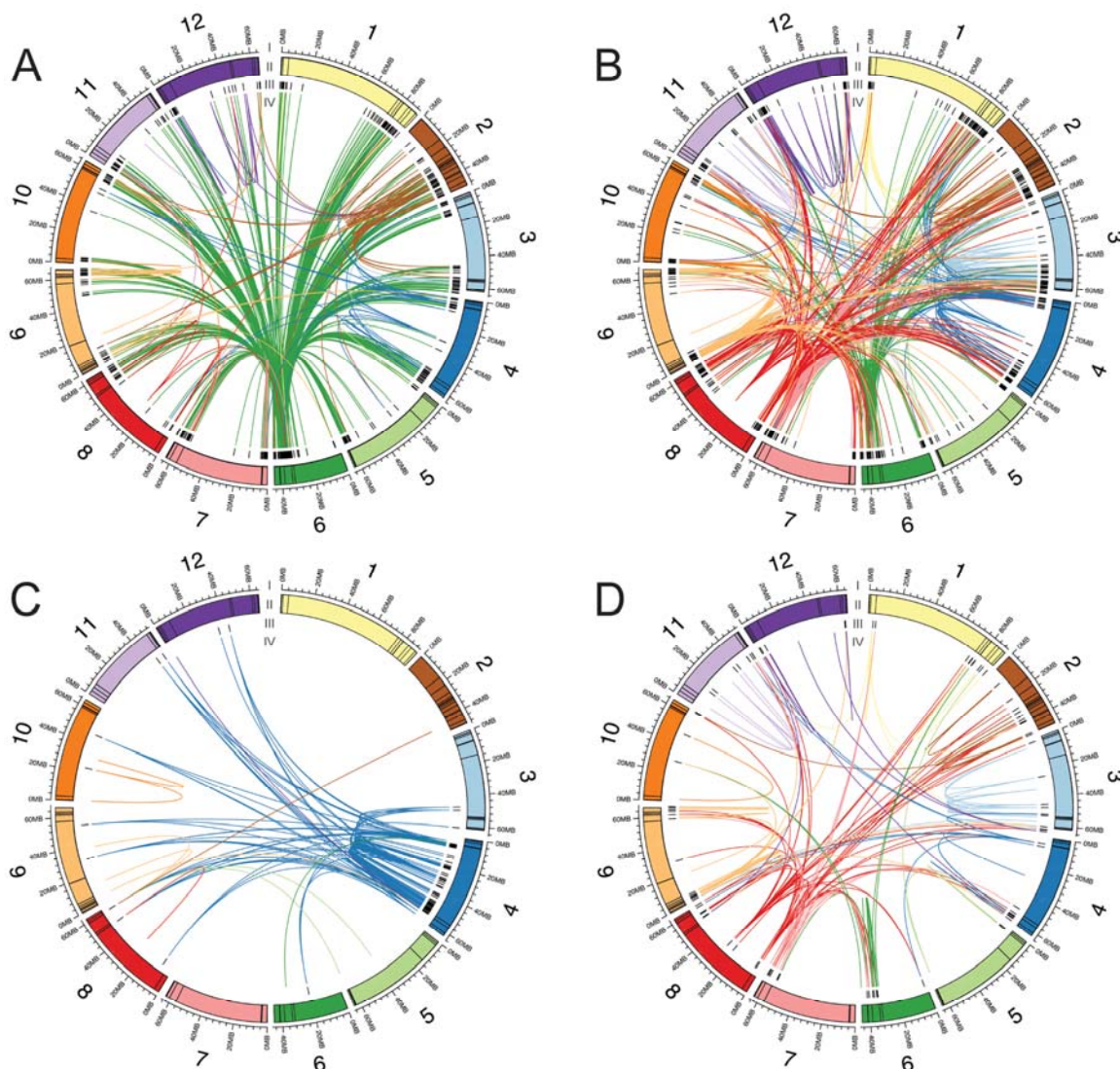


Figure 4. Connections between eQTL and the genes they regulate. Each plot includes the genes with eQTL that were clustered together into a module based on expression patterns. A) Defense module. B) Photosynthesis module. C) Cysteine peptidase module. D) Leaf development module. I) The 12 tomato chromosomes in megabases. II) Colored boxes indicate the sizes of each bin. III) Black bars indicate the locations of the genes. IV) Chords connect eQTL to the genes whose expression patterns they regulate. Chords are colored by the chromosome location of the eQTL.

319 species; this cluster was uniquely associated with *S. pennellii* orthologs at the P5
 320 stage of leaf development, indicating that this species has a unique pattern of
 321 gene expression, which involves peptidase regulation (Ichihashi et al., 2014) and
 322 may be related to leaf senescence processes (Diaz-Mendoza et al., 2014).

323

324 **Genetic regulation of transcriptional responses associated with plant**
325 **defense**

326 One of the landmark modules from the clustering analysis was enriched
327 for gene expression patterns related to plant defense (Figure 3B; Supplemental
328 Dataset 7). Therefore we explored the genetic basis of transcriptional changes
329 associated with plant defense. IL6.2 and IL6.2.2, in particular, influence the
330 transcriptional responses of genes associated with plant defense and signaling
331 (Supplemental Dataset 1). The overlapping regions between IL6.2 and IL6.2.2,
332 bins 6B and 6C, also have the largest numbers of *trans*-eQTL (Figure 4A). The
333 genes showing increased expression in both ILs compared to cv. M82, as well as
334 the genes regulated by the corresponding bins, show enrichment of the GO
335 categories response to stress and stimulus, cell death, defense response, and
336 plant-type hypersensitive response (Supplemental Dataset 9 and 10). Promoter
337 enrichment analysis for these genes showed enrichment of a W-box promoter
338 motif that is recognized by WRKY transcription factors and influences plant
339 defense response (Supplemental Dataset 11 and 12) (Yu et al., 2001). Both the
340 bins, in particular bin 6C, contain genes involved in pathogen, disease, and
341 defense response: such as *NBS-LLR resistance genes*, *WRKY transcription*
342 *factors*, *Multidrug resistance genes*, *Pentatricopeptide repeat-containing genes*,
343 *Chitinase*, and *Heat Shock Protein* coding genes. These genes are known to
344 influence plant defense responses at a global transcriptome level. The
345 transcriptional response in the ILs is also reflected in the morphology of IL6.2.2;

346 the plants are necrotic and dwarfed (http://tgrc.ucdavis.edu/pennellii_ils.aspx,
347 (Sharlach et al., 2013). A bacterial spot disease resistance locus from *S. pennellii*,
348 *RXopJ4*, that confers hypersensitive response in IL6.2 and 6.2.2, has been
349 mapped to 190Kb region in bin 6C (Sharlach et al., 2013). In addition IL 4.1, 5.2,
350 8.1.1, and 9.1.3 also showed DE of genes involved in plant defense response,
351 though the effect of was not as strong as that of IL6.2 and 6.2.2. Taken together,
352 these findings suggest bins 6B and 6C contain master genetic regulators of plant
353 defense response genes, though identification of the causal gene/s that influence
354 so many other genes in *trans* will need further genetic dissection of these bins.

355

356 **Genetic regulation of transcriptional responses associated with leaf** 357 **development**

358 Given the striking differences in leaf features between *Solanum pennellii*
359 and cv. M82 that are manifested in many ILs (Chitwood et al., 2013), the IL
360 population provides an excellent system for determining the extent of genetic
361 regulation on leaf developmental genes. Moreover the tissues used for
362 transcriptomic analyses included developing leaves and leaf primordia. Therefore
363 we examined the effect of individual introgressions and associated bins on leaf
364 developmental genes. Previous phenotypic and QTL analyses identified many
365 ILs, such as IL4.3, IL8.1.5, IL8.1.1, and IL8.1, harboring loci regulating leaf and
366 plant developmental traits (Holtan and Hake, 2003; Chitwood et al., 2013; Muir et
367 al., 2014). IL4.3 harbors loci with the largest contribution to leaf shape, which
368 manifests as larger epidermal cell size and reduced leaf complexity (Chitwood et

369 al., 2013). This IL shows decreased expression of many genes encoding proteins
370 involved in cell division, such as Cyclin-dependent protein kinase regulator-like
371 protein (CYCA2;3), Cyclin A-like protein (CYCA3;1), CYCLIN B2;3, and F-
372 box/LRR-repeat protein 2 SKP2A (Supplemental Dataset 9). In addition, IL4.3
373 regulated genes were enriched for the promoter motifs MSA (M-specific
374 activators that are involved in M-phase specific transcription) and the E2F
375 binding site (Supplemental Dataset 11). Down-regulated genes in ILs 8.1.5,
376 8.1.1, and 8.1, also included leaf development and morphology genes, including
377 genes encoding WD-40 repeat family protein LEUNIG, Homeobox-leucine zipper
378 protein PROTODERMAL FACTOR 2, and the transcription factor
379 ULTRAPETALA (Supplemental Dataset 9; Abe et al., 2003; Cnops et al., 2004;
380 Carles et al., 2005). However target genes for none of the individual eQTL
381 showed GO enrichment associated with leaf development categories
382 (Supplemental Dataset 10). This could, in part, be due to complexity of the tissue
383 used for RNAseq analysis, as the mixture of shoot apical meristem, growing
384 leaves and hypocotyl could have diluted the significant leaf developmental genes.

385 As an alternative, we investigated the expression dynamics of a set of
386 literature-curated leaf developmental genes (Ichihashi et al., 2014) across the ILs,
387 to locate the hotspots regulating these genes (Supplemental Dataset 13). A
388 number of canonical leaf developmental genes such as *SHOOT*
389 *MERISTEMLESS* (Solyc02g081120, *STM*), *GROWTH-REGULATING FACTOR*
390 *1* (*GRF1*, Solyc04g077510), *ARGONAUTE 10* (*AGO10*, Solyc12g006790), *BELL*
391 (*BEL1*, Solyc08g081400) *LEUNIG* (Solyc05g026480) and *SAWTOOTH 1* (*SAW1*,

392 Solyc04g079830) were differentially expressed in more than five ILs. At the level
393 of bins, genes involved in leaf development were seen to be regulated by eQTL
394 scattered widely across the genome (Figure 4D). This underscores the highly
395 polygenic regulation of leaf development (Chitwood et al., 2013) as multiple loci,
396 residing in many different chromosomal locations, regulate the expression of key
397 leaf-developmental genes. Fifty-eight of literature-curated leaf developmental
398 genes have expression patterns under eQTL regulation; three bins (2G, 7H, 8A)
399 each have four significant eQTL regulating leaf developmental genes, which is
400 the maximum number for any bin (Figure 4D, Supplemental Dataset 14). Bin 8A,
401 the overlapping region of IL8.1, 8.1.1, and 8.1.5, contains *LEUNIG* that showed a
402 200-fold down-regulation in the differential gene expression analysis for the three
403 ILs (Supplemental Dataset 1). Bin 8A, further, contains *trans*-eQTL that regulate
404 the expression pattern of key auxin-related genes, such as *AINTEGUMENTA*
405 (*ANT*; Solyc04g077490), and *YUCCA4* (Solyc06g065630; Supplemental Dataset
406 14). Consistent with this, IL 8.1.1, 8.1.5 and 8.1 have strong reduction in leaf
407 complexity in the direction of *S. pennellii* (Chitwood et al., 2013). Similarly IL4.3
408 contains loci with the largest contributions to leaf shape variation (Chitwood et al.,
409 2013), and also regulates the *TCP5* gene in *trans*.

410 BH-SNE clustering corroborated the strong leaf phenotypes for ILs 4.3,
411 8.1, 8.1.1, and 8.1.5. We compared a curated list of leaf developmental genes
412 combined with a set of co-expressed genes (LC+; (Ichihashi et al., 2014)) to the
413 3,592 genes found within the identified modules in the BH-SNE mapping (Figure
414 3). A total of 175 genes out of 697 from the list were found within the modules;

415 the highest concentrations were 108 genes located in the photosynthesis module
416 and 19 in the leaf development module (Supplemental Figure S7B; Supplemental
417 Dataset 15 and 16), suggesting a relationship between these two modules. The
418 eQTL regulating expression patterns of these leaf developmental genes were
419 distributed broadly across the genome (Supplemental Figure S7A, Supplemental
420 Dataset 17). This is consistent with the differential expression and eQTL
421 analyses, which found that no one bin or IL regulates leaf developmental genes.
422 Over one third of the gene expression patterns in the leaf development module
423 have significant eQTL that map to bins 4D, 8A, and 8B (5.4%, 16.2%, and 15.5%,
424 respectively), suggesting that these bins contain important regulators of leaf
425 development. The canonical leaf developmental genes within this module
426 include: *GROWTH-REGULATING FACTOR7* (*GRF7*; Solyc03g082430); *GRF10*
427 (Solyc09g009200); *ERECTA-LIKE 1* (Solyc03g007050, *ERL1*); *ARGONAUTE 10*
428 (Solyc12g006790, *AGO10*); *AUXIN RESPONSE FACTOR 9* (Solyc08g008380,
429 *ARF9*); and *AINTEGUMENTA* (Solyc04g077490, *ANT*). Altogether DE, eQTL
430 and BH-SNE results indicate that while there is no obvious master regulatory bin
431 for leaf developmental genes, many are under strong genetic regulation by eQTL
432 distributed throughout the genome (Figure 4D).

433

434 **Genetic regulation of transcriptional responses associated with** 435 **photosynthesis**

436 Since photosynthesis GO terms were enriched for the largest module from
437 the clustering analysis (Figure 3B) and there was a correlation between

438 photosynthesis and leaf developmental modules (Supplemental Figure S7B), we
439 examined the genetic regulation of photosynthetic genes by specific ILs and
440 corresponding bins. Genes related to photosynthesis show increased expression
441 across 21 ILs distributed on all chromosomes except chromosome 5
442 (Supplemental Dataset 9), showing multigenic regulation of these critical traits.
443 Many of these ILs, including 8.1.5, 8.1.1, and 8.1, which share an introgressed
444 region, and IL4.3, have up-regulated genes enriched for the GO-categories
445 photosynthesis, chlorophyll biosynthesis, and response to light stimulus
446 (Supplemental Dataset 9). The eQTL target genes of corresponding bins 4D and
447 8A also have GO enrichments for photosynthesis (Supplemental Dataset 10).
448 These ILs also had significant effects on leaf shape and morphology (Chitwood
449 et al., 2013). Previously we reported a link between leaf development and
450 photosynthesis by meta-analysis of developmental and metabolic traits
451 (Chitwood et al., 2013). This indicates that ILs may also differ from each other
452 and from cultivated M82 background in photosynthetic efficiency. However no
453 studies, so far, has investigated the photosynthetic phenotype of these ILs.

454 To analyze this relationship between the leaf development and
455 photosynthesis modules the median expression value of all genes in each
456 module was compared resulting in a significant negative correlation (adj r^2 =
457 0.77; Figure 5). The transition from leaf development to leaf maturation is
458 potentially reflected in our data. The genes found in the leaf development module
459 may promote developmental processes such as cell division and maintenance or
460 meristematic potential, whereas the leaf development related genes found in the

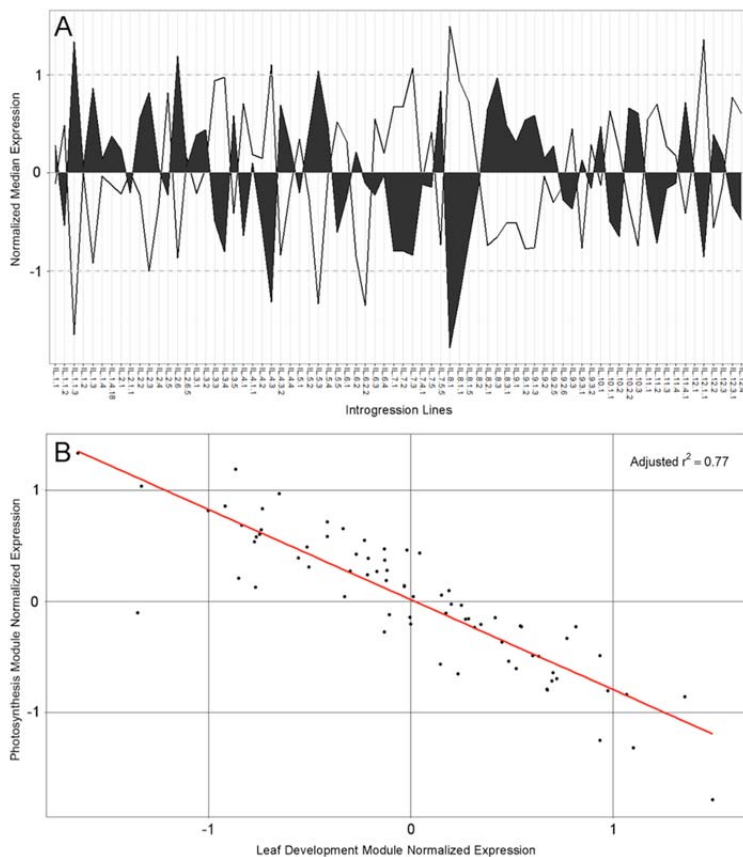


Figure 5. Median expression values for leaf development and photosynthesis related modules and expression correlation. (A) The median expression values of a module for each IL are shown. A consistent negative correlation between photosynthesis and Leaf development transcript expression is evident across nearly all 74 ILs. Dashed lines indicate one significant deviation from the module mean expression. Filled areas represent the median expression of the leaf development module, while open areas indicate the photosynthesis module median expression. (B) Leaf development median expression versus photosynthesis median expression values for each IL show a distinct negative correlation with an adjusted R-squared value of 0.77 (calculated by linear regression in R).

461 photosynthesis module may act to suppress this process to allow for maturation
462 of the leaf. The strong negative correlation between the expression patterns of
463 these two modules (Figure 5) and the overlap between their most influential
464 eQTLs (Supplemental Figure S7A; Supplemental Table III) suggests that leaf
465 development and photosynthetic genes not only have expression levels in
466 opposition but also likely share common regulatory loci. Each module has eQTLs
467 on bins 4D, 8A, and 8B which may indicate these regions drive the regulatory
468 “switch” from development to maturation and photosynthetic activity.

469

470 **Dissection of identified eQTL to spatially- and temporally- regulated**
471 **development**

472 The significant eQTL detected in this study represent the genetic
473 regulation of gene expression in the tomato shoot apex that includes shoot apical
474 meristem (SAM) and developing leaves. Using previous gene expression data,
475 we spatio-temporally resolved the detected eQTL to specific tissues and
476 temporally-regulated development. We analyzed gene expression in laser micro-
477 dissected samples representing the shoot apical meristem (SAM) + P0 (the
478 incipient leaf) vs. the P1 (the first emerged leaf primordium) (Figure 6A) and hand
479 dissected samples of the SAM + P0-P4 vs. the P5 collected over time (Figure 6B-
480 C), representing genes regulated by vegetative phase change (heteroblasty)
481 (Chitwood et al., 2015). The former dataset represents gene expression in the
482 meristem (SAM) and the first differentiated leaf (P1), whereas the latter dataset
483 informs about gene expression changes during the temporal development of the
484 shoot apex.

485 Using a bootstrapping approach, we identified bins statistically enriched
486 for genetically regulating genes with previously identified gene expression
487 patterns (Figure 6D-F). Except for one instance (cis-regulated genes with high
488 SAM/P0 expression located in bin 2I), bins enriched for gene expression patterns
489 represented *trans* regulation, hinting at predominately transcription factor-based
490 regulation of gene expression patterns. Most SAM/P0 vs. P1 enriched bins were
491 enriched for P1 gene expression (Figure 6D). We previously showed that genes
492 with high P1 expression are enriched for photosynthetic-related GO terms,

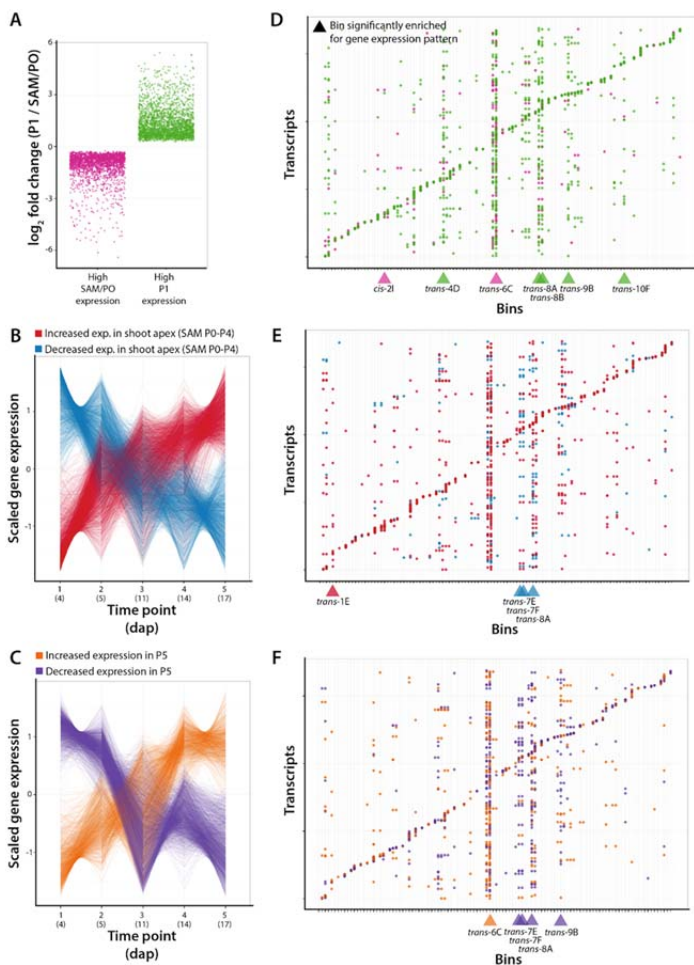


Figure 6. Enriched expression patterns for genes genetically regulated by bins.

A) Log fold change values (P1/SAM+P0) for previously identified differentially expressed genes with high expression in the SAM + P0 (magenta) vs. P1 (green). B) Scaled gene expression values for previously identified differentially expressed genes with increasing (red) and decreasing (blue) expression over developmental time in the SAM + P0-P4. C) Scaled gene expression values for previously identified differentially expressed genes with increasing (orange) and decreasing (purple) expression over developmental time in P5. D) Transcripts (y-axis) and bins (x-axis) showing the genetic regulation of gene expression (eQTL). Colors indicate SAM + P0 (magenta) and P1 (green) transcripts. Bins enriched for genetically regulating genes with specific expression patterns are indicated below with triangles. E) Same as in D), except showing genes with increasing (red) and decreasing (blue) expression over temporal time in the SAM + P0-P4. F) Same as in D), except showing genes with increasing (orange) and decreasing (purple) expression over temporal time in P5. Previously determined gene expression patterns are previously published (Chitwood et al., 2015).

493 compared to SAM/P0 genes enriched for transcription, cell division, and
 494 epigenetics-related GO terms (Chitwood et al., 2015), suggesting a genetic basis
 495 at both a functional and tissue-specific level for genes related to photosynthesis
 496 expressed preferentially in the P1 compared to the SAM/P0. Of bins enriched for
 497 SAM/P0 vs. P1 gene expression patterns, bins 4D, 8A, and 9B were significantly
 498 enriched for photosynthetic-related GO terms, indicating that these bins in

499 particular contain eQTL important for the regulation of photosynthetic processes
500 (Supplemental Dataset S18).

501 Bins enriched for regulation of genes with temporally-dependent
502 expression were mostly associated with genes with decreasing expression over
503 time, for both the SAM + P0-P4 and P5 (Figure 6E-F). Interestingly, 3 bins (7E,
504 7F, and 8A) share enrichment for genes with decreasing expression patterns
505 over time in both the SAM + P0-P4 and P5 (Figure 6E-F), suggesting true
506 temporal *trans* regulation, regardless of tissue, by these loci. Broadly, genes with
507 increasing expression over time are associated with transcription and small RNA
508 GO terms in both the SAM + P0-P4 and P5, whereas decreasing expression over
509 time is associated with translation associated GO terms in the SAM + P0-P4 and
510 photosynthetic activity in the P5. Specifically bin 6C, which was enriched for
511 genes with increasing expression over time for P5, was also significantly
512 enriched for defense processes GO terms; whereas bins 8A and 9B, that showed
513 enrichment for genes with decreasing patterns over time for P5, were enriched
514 for photosynthesis-related GO terms (Supplemental Dataset S18).

515

516 **Linking leaf and hypocotyl phenotypes to detected eQTL**

517 To better understand genetic regulation of gene expression itself, eQTL
518 provide crucial links between genetic loci and organism level phenotypes, often
519 generated in diverse tissue/organ types and environments. The tissue samples
520 used for our transcriptomic analyses contained developing leaves and hypocotyl.
521 Therefore, in order to connect detected eQTL with leaf and hypocotyl phenotypes

522 under two different environmental conditions, we correlated gene expression with
523 leaf number, leaf complexity (as measured in Chitwood et al., 2014) and
524 hypocotyl length phenotypes of the ILs grown under simulated sun and shade
525 conditions. Significant correlations with gene expression patterns were identified
526 for all three phenotypes analyzed under both treatments (Supplemental Table IV).
527 Focusing on a subset of these gene expression patterns that had associated
528 eQTL enabled us to connect the phenotypes to their regulatory loci
529 (Supplemental Table IV).

530 Genes negatively correlated with leaf number showed enrichment of leaf
531 development GO terms, whereas positively correlated genes showed enrichment
532 of photosynthesis-related GO terms (Supplemental Figure S8A-B; Supplemental
533 Dataset 2 in Chitwood et al., 2014). The expression pattern of these genes
534 associated with leaf number was predominantly regulated by eQTL on
535 chromosomes 7 and 8 (Supplemental Figure S8C-D) and reveals developmental
536 transitions reflecting a shift from leaf development to photosynthetic activity with
537 the increase in leaf number and plant maturity. For the leaf complexity trait,
538 correlations were reversed compared to leaf number, and a positive correlation
539 with genes enriched for leaf development and negative correlation with
540 photosynthesis genes was seen (Supplemental Figure S9A-B; Supplemental
541 Dataset 19). Moreover a larger number of correlations with leaf developmental
542 gene expression patterns were observed for leaf complexity in response to shade
543 (Supplemental Figure S9C-D; Supplemental Table IV). This reflects the higher
544 leaf complexity observed in shade-grown tomato plants (Xu et al., 2009;

545 Chitwood et al., 2015). eQTL on chromosomes 4, 7 and 8 were primarily involved
546 in regulation of gene expression patterns associated with leaf complexity
547 (Supplemental Figure S9C-D). These results, in combination with DE, eQTL and
548 BH-SNE, highlight bins on chromosomes 4 and 8 as important genetic regulators
549 of leaf developmental genes.

550 Five genes were positively correlated with hypocotyl length under
551 simulated shade and only one gene (Solyc10g005120) was negatively correlated
552 with hypocotyl length under both sun and shade (Figure 7A; Supplemental
553 Dataset 20). eQTL for the positively correlated genes are located on
554 chromosomes 3, 7, and 11, whereas the single cis-eQTL for the negatively
555 correlated gene, Solyc10g005120 (an uncharacterized *Flavanone 3-hydroxylase-*
556 *like* gene), was located in bin 10A.1 (Supplemental Figure S10; Figure 7B). The
557 gene is only expressed in IL 10.1, which has the *S. pennellii* copy of the gene,
558 and not in other ILs with the M82 version of the gene, such as IL 10.1.1. Further,
559 M82 and IL 10.1.1 showed significant elongation of hypocotyls in response to
560 shade, whereas IL 10.1 had an attenuated shade avoidance response
561 (Supplemental Figure S11). This indicates the influence of genes exclusively in
562 this introgression on hypocotyl length, specifically those located in bin 10A that
563 includes Solyc10g005120. A set of BIL (Backcross Inbred Lines) lines generated
564 in a new mapping population developed from the same parents, cv. M82 and *S.*
565 *pennellii*, provides higher resolution gene mapping as bin sizes are significantly
566 smaller (Muller et al., 2016; Fulop et al., In Review). BIL-128 harbored a smaller
567 introgression on chromosome 10 compared to IL 10.1, carried the *S. pennellii*

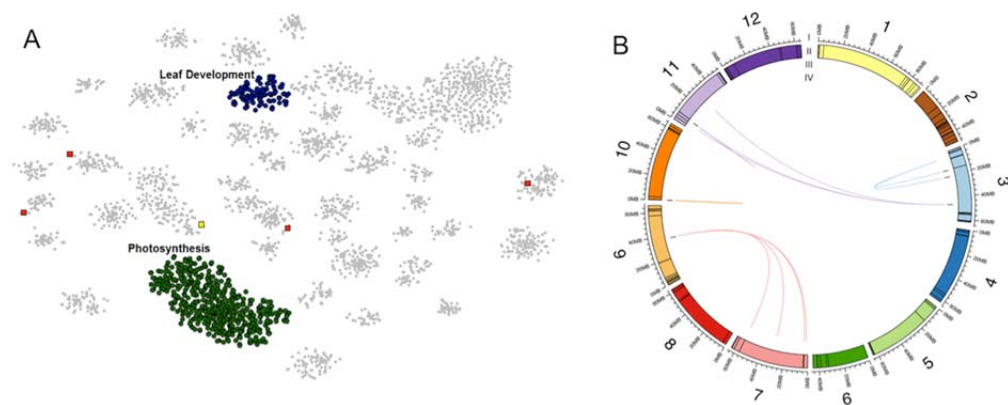


Figure 7. eQTL regulation of gene expression patterns that correlate with hypocotyl length.
A) Forty-two distinct modules identified by DBscan from the eQTL mapping generated by BH-SNE analysis. Modules enriched for genes with leaf development and photosynthesis GO terms are labeled in blue and green, respectively. Genes with expression patterns correlated with hypocotyl length under simulated shade are indicated by squares with positive correlations in red and negative correlations in yellow.
B) Genes with expression patterns correlated with hypocotyl length under simulated shade are shown connected to their respective eQTL with chords. I) The 12 tomato chromosomes in megabases. II) Colored boxes indicate the sizes of each bin. III) Black bars indicate the locations of the genes. IV) Chords connect eQTL to the genes whose expression patterns they regulate. Chords are colored by the chromosome location of the eQTL.

568 version of Solyc10g005120, and resembled IL10.1 in its hypocotyl length in
569 response to shade (Supplemental Figure S10; S11). However, it had an
570 additional introgression on chromosome 2. BIL-033 that shared an overlapping
571 introgression with BIL-128 on chromosome 2 showed a hypocotyl phenotype
572 similar to M82, ruling out the possibility of influence of chromosome 2 genes on
573 the hypocotyl phenotype (Supplemental Figure S10; S11). Though the function of
574 Solyc10g005120 has not been described for Arabidopsis or tomato so far, our
575 gene expression and phenotypic observations present it as a new potential
576 candidate for further exploring the regulation of hypocotyl length and other plant
577 phenotypes in response to shade.

578

579 **Transgressive expression of genes among ILs**

580 Interspecific crosses combining divergent genomes can sometimes result
581 in improved performance. Transcriptomic studies of wild and resynthesized
582 hybrids show extensive gene expression alterations in the hybrids compared to
583 their parents (Hegarty et al., 2008). The IL population allows us to study the
584 combination of divergent genomes across many genetically distinct lines. Many
585 of the changes we see are “transgressive”, falling outside the range seen in
586 either parent. A total of 2,286 genes, more than one fourth of unique DE genes
587 between the ILs and cv. M82, showed transgressive expression patterns, i.e.
588 genes were differentially expressed for the IL but not for *S. pennellii* compared to
589 cv. M82 (Supplemental Dataset 21). These genes were distributed across all ILs
590 but the extent of transgressive gene expression varied among the ILs. ILs with
591 high number of differentially expressed genes, such as IL6.2.2, IL4.3, and IL8.1,
592 also showed higher number of transgressively expressed genes (Supplemental
593 Figure S12A). While synthetic allotetraploids generated from interspecific crosses
594 show large scale down regulation of gene expression (likely due to silencing of
595 duplicate gene copies (Wang et al., 2006)) and the affected genes fall in the
596 categories of cell defense, ageing and hormonal regulation, the transgressive
597 genes in this IL population generated by interspecific crossing show mostly
598 upregulation of gene expression with genes falling in the broad categories of
599 photosynthesis, energy metabolism, microtubule movement, and extrinsic
600 membrane components (Supplemental Dataset 22). In order to estimate the
601 relative effect of the introgression on transgressive gene expression, we
602 quantified the ratio of the number of genes with transgressive expression to the

603 number of genes with *S. pennellii* like expression (*transgressive_to_S. pennellii*-
604 like) for each IL (Supplemental Figure S12B). A few ILs, such as IL1.4.18, IL4.3,
605 IL7.3, IL8.1, IL11.1, and IL12.1.1, showed a *transgressive_by_S. pennellii* value
606 greater than 0.5, suggesting a higher effect of the corresponding introgression on
607 gene expression in M82 background. Most of the transgressively expressed
608 genes for each IL were located in *trans*, beyond the introgression region
609 (Supplemental Figure S12A). These may result from novel combinations of
610 regulatory factors (Riddle and Birchler, 2003), recombination of alleles present at
611 different loci in the parent species through complementary gene action
612 (Rieseberg et al., 1999), more abundant production of small interfering (si) RNAs
613 in progeny of interspecific crosses than in either parent with concomitant
614 suppression of the corresponding target genes, and hypermethylation of the
615 corresponding genomic DNA (Shivaprasad et al., 2012).

616

617 **Conclusion**

618 In this study we have investigated the regulation of gene expression in the
619 progeny of crosses between cultivated tomato (*Solanum lycopersicum* cv. M82)
620 and a wild relative (*Solanum pennellii*, accession LA716). A combination of
621 differential gene expression, eQTL, and clustering analyses provide a
622 comprehensive picture of genetic regulation of transcript expression patterns in
623 this IL population. We show differential genetic effects of discrete genomic
624 regions that regulate gene expression patterns. Certain regions are highly active,
625 particularly those on chromosome 4, 6, and 8, and they influence the expression

626 patterns of genes in their own introgression regions and beyond. Clustering of
627 genes by expression patterns and GO/promoter motif enrichment analyses
628 provided further insights into the genetic regulation of expression patterns of
629 genes related to specific pathways. Our data show that some biological pathways,
630 such as plant defense, are under the regulation of a limited number of loci with
631 strong effects, whereas loci regulating other pathways, such as photosynthesis
632 and leaf development, are scattered throughout the genome most likely with
633 weaker individual effects. Using published gene expression atlases for tomato we
634 were able to partition the eQTLs into tissue specific and age dependent patterns
635 of expression. We correlated gene expression with leaf and hypocotyl
636 phenotypes and identified the regulatory regions driving these gene expression
637 patterns. In the case of hypocotyl length we identified a strong candidate gene
638 that may regulate hypocotyl length under shade avoidance. This is the first
639 comprehensive insight into the global regulation of transcript abundance in
640 tomato and sets the stage for identification of gene/s underlying these regulatory
641 loci. Coupled with comprehensive phenotyping on these ILs this data set
642 provides insights into how the expression pattern of key genes or gene modules
643 can be genetically manipulated to achieve a desirable plant phenotype. We
644 report on differential gene expression between the ILs and the recurrent parent,
645 M82, eQTLs that regulate these gene expression patterns and transgressive
646 changes in gene expression. Together these facets of change in gene
647 expression may explain hybrid performance, and could provide genotypes that
648 have an enhanced ability to survive in habitats not accessible to the parents.

649 While they may provide avenues for enhancing breeding efforts, they also reveal
650 unexpected consequences of wide crosses. A study of transcriptional variation is
651 only one component of many others, such as protein and metabolite levels, to
652 influence downstream phenotypes. Given a number of important plant traits have
653 complex inheritance, transcript abundance can function as an intermediate
654 between genomic DNA sequence variation and complex traits. Our ability to
655 predict and understand the downstream effects of genes introgressed from wild
656 relatives on gene expression patterns and ultimately phenotypes will be a critical
657 component of crop plant enhancement.

658

659

660 **Materials and Methods**

661 **Plant Materials, Growth Conditions, and Experimental Design**

662 Plant materials, growth conditions, and experimental design were described in
663 (Chitwood et al., 2013), but are outlined here briefly. Seeds of *Solanum pennellii*
664 ILs (Eshed and Zamir, 1995; Liu and Zamir, 1999) and *Solanum lycopersicum* cv.
665 M82 were obtained either from Dani Zamir (Hebrew University, Rehovot, Israel)
666 or from the Tomato Genetics Resource Center (University of California, Davis).
667 Seeds were stratified in 50% bleach for 2 min., grown in darkness for 3 d for
668 uniform germination before moving to a growth chambers for 5 days. Six
669 seedlings of each genotype were planted per pot for each replicate. The 76 ILs
670 (and two replicates each of cv. M82 and *S. pennellii*) were divided into four
671 cohorts of 20 randomly assigned genotypes. These cohorts were placed across

672 four temporal replicates in a Latin square design as described in (Chitwood et al.,
673 2013). The seedlings were harvested 5 d after transplanting (13 d of growth in
674 total). Cotyledons and mature leaves >1 cm in total length were excluded, and
675 remaining tissues (including the shoot apical meristem) above the midpoint of the
676 hypocotyl were pooled, for all individuals in a pot, into 2-mL microcentrifuge
677 tubes and immediately frozen in liquid nitrogen. Two ILs, IL7.4 and IL12.4.1 were
678 not included in the final analysis due to seed contaminations.

679

680 **Growth conditions and quantification of hypocotyl length**

681 Seeds 76 ILs along with the parents were sterilized using 70% ethanol,
682 followed by 50% bleach, and finally rinsed with sterile water. This experiment
683 was replicated three times each in 2011 and 2012. Ten to twelve seeds of each
684 IL were sown into Phytatray II (Sigma-Aldrich) containers with 0.5x Murashige
685 and Skoog minimal salt agar. Trays were randomized and seeds germinated in
686 total darkness at room temperature for 48h. Trays of each IL were randomly
687 assigned to either a sun or shade treatment consisting of 110 μ Mol PAR with a
688 red to far-red ratio of either 1.5 (simulated sun) or 0.5 (simulated shade) at 22°C
689 with 16 hour light / 8 hour dark cycles for 10d. Three genotypes were excluded
690 from the analyses due to poor germination (IL3.3) or their necrotic dwarf
691 phenotypes (IL6.2, 6.2.2). After 10d, seedlings were removed from the agar and
692 placed onto transparency sheets containing a moistened kimwipe to prevent
693 dehydration and scanned using an Epson V700 at 8-bit grayscale at 600 dpi.
694 Image analysis was carried out using the software ImageJ (Abramoff et al., 2004).

695 For hypocotyl length analysis of backcross inbred lines between *S.*
696 *pennellii* and *S. lycopersicum* cv. M82, seeds were sterilized in 50% bleach and
697 then rinsed with sterile water. They were then placed in Phytatrays in total dark at
698 room temperature for 72 hours, and then moved to 16 hour light / 8 hour dark for
699 4d. Seedlings were transferred to soil using a randomized design and assigned
700 to either a sun or shade treatment (as described above) for seven days. Images
701 were taken with a HTC One M8 Dual 4MP camera and hypocotyl lengths
702 measured in ImageJ (Abramoff et al., 2004) using the Simple Neurite Tracer
703 (Longair et al., 2011) plugin.

704

705 **Correlation of phenotype with gene expression pattern**

706 Gene expression patterns were correlated with three phenotypes collected
707 from the ILs along with the parents. Normalized estimated read counts with 3-4
708 independent replicates per IL were log2 transformed prior to the analyses. Leaf
709 number and leaf complexity were collected from the ILs as outlined in Chitwood
710 et al. (2014) under both sun and shade treatments. Hypocotyl lengths were
711 measured as detailed above. To test whether a gene's expression pattern was
712 correlated with a particular phenotype bootstrapping analyses were performed.
713 Expression and phenotype data were randomly permuted (with replacement)
714 using the `sample()` function against IL and then merged. For each analysis, 1000
715 replications were performed and the p-values were calculated from the
716 Spearman's rho value distributions. P-values were adjusted for multiple
717 comparisons using the BH correction (Benjamini & Hochberg, 1995). Significant

718 correlations were identified as those with an adjusted p-value < 0.05 and the
719 mean rho value (the correlation coefficient) was used to designate the correlation
720 as either positive (positive slope) or negative (negative slope). All analyses were
721 implemented using the statistical software R and custom scripts (R Core Team,
722 2015).

723

724 **RNA-Seq Library Preparation and Preprocessing RNA-Seq Sequence Data**

725 RNAseq libraries were prepared and the reads were preprocessed as described
726 in (Chitwood et al., 2013), and are outlined here. mRNA isolation and RNA-Seq
727 library preparation were performed from 80 samples at a time using a high-
728 throughput RNA-Seq protocol (Kumar et al., 2012). The prepared libraries were
729 sequenced in pools of 12 for replicates 1 and 2 (one lane each) and in pools of
730 80 for replicates 3 and 4 (seven lanes) at the UC Davis Genome Centre
731 Expression Analysis Core using the HiSeq 2000 platform (Illumina).
732 Preprocessing of reads involved removal of low quality reads (phred score < 20),
733 trimming of low-quality bases from the 3' ends of the reads, and removal of
734 adapter contamination using custom Perl scripts. The quality-filtered reads were
735 sorted into individual libraries based on barcodes and then barcodes were
736 trimmed using custom Perl script.

737

738 **Read Mapping and Gene Expression Analysis**

739 Mapping and normalization were done on the iPLANT Atmosphere cloud server
740 (Goff et al., 2011). *S. lycopersicum* reads were mapped to 34,727 tomato cDNA

741 sequences predicted from the gene models from the ITAG2.4 genome build
742 (downloadable from
743 ftp://ftp.solgenomics.net/tomato_genome/annotation/ITAG2.4_release/). A
744 pseudo reference list was constructed for *S. pennellii* using the homologous
745 regions between *S. pennellii* scaffolds v.1.9 and *S. lycopersicum* cDNA
746 references above. Using the defined boundaries of ILs, custom R scripts were
747 used to prepare IL-specific references that had the *S. pennellii* sequences in the
748 introgressed region and *S. lycopersicum* sequences outside the introgressed
749 region. The reads were mapped using BWA (Li and Durbin, 2009; Roberts and
750 Pachter, 2013) using default parameters except for the following that were
751 changed: `bwa aln: -k 1 -l 25 -e 15 -i 10` and `bwa samse: -n 0`. The bam alignment
752 files were used as inputs for `express` software to account for reads mapped to
753 multiple locations (Roberts and Pachter, 2013). The estimated read counts
754 obtained for each gene for each sample from `express` were treated as raw counts
755 for differential gene expression analysis. The counts were then filtered in R using
756 the Bioconductor package `EdgeR` version 2.6.10 (Robinson and Oshlack, 2010)
757 such that only genes that have more than two reads per million in at least three
758 of the samples were kept. Normalization of read counts was performed using the
759 trimmed mean of M-values method (Robinson and Oshlack, 2010), and
760 normalized read counts were used to identify genes that are differentially
761 expressed in each IL compared to cv. M82 parent as well as in between two
762 parents, *S. pennellii* and M82. The DE genes for each IL were compared to those
763 between the two parents to identify genes that were differentially expressed for

764 the IL but not for *S. pennellii* compared to cv. M82. Those genes were
765 considered to show transgressive expression pattern for the specific IL, whereas
766 other DE genes were considered to show *S. pennellii* like expression pattern.

767

768 **Methods for eQTL Analyses**

769 eQTL mapping analyses were performed to determine whether the expression
770 pattern of a gene is correlated with the presence of a specific introgression from
771 *S. pennellii* into *S. lycopersicum* cv. M82. This was examined at the level of “bin”,
772 with a bin defined as a unique overlapping region between introgressions.
773 Examining eQTL at the bin level enables them to be mapped to considerably
774 smaller intervals than the ILs themselves (Liu and Zamir, 1999). eQTL mapping
775 analyses were performed on the normalized estimated read counts with 3-4
776 independent replicates per IL, which were log2 transformed prior to the analyses.
777 To test whether a gene’s expression pattern is correlated with the presence of a
778 particular bin a Spearman’s rank correlation test was used with ties resolved
779 using the midrank method. P-values were adjusted for multiple comparisons
780 using the BH correction (Benjamini and Hochberg, 1995). Significant eQTL were
781 identified as those with an adjusted p-value < 0.05 and Spearman’s rho (the
782 correlation coefficient) was used to designate the eQTL as up (positive slope) or
783 down (negative slope). All analyses were implemented using the statistical
784 software R and custom scripts (R Core Team, 2015).

785

786 **Methods for eQTL clustering analysis**

787 **Data Preparation:** In preparation for analysis using the Barnes-Hut-SNE
788 algorithm the data set was log2 transformed. Each gene's expression profile was
789 then normalized across all 74 introgression lines so that the profile had a mean of
790 zero and a standard deviation of one. Normalization of the data allowed for
791 comparison of the relative relationship between each gene expression profile
792 (Bushati et al., 2011).

793 **Barnes-Hut-SNE:** *t*-SNE or *t*-distributed stochastic neighbor embedding (van
794 der Maaten and Hinton, 2008) is a non-linear dimensionality reduction method,
795 which faithfully maps objects in high dimensional space (H-space) into low
796 dimensional space (V-space). Crowding is avoided through the long-tailed *t*-
797 distribution, which forces non-neighbor clusters farther away from each other in
798 V-space than they actually are in H-space (van der Maaten and Hinton, 2008).
799 The exaggerated separation of non-neighboring clusters improves 2D resolution,
800 allowing identification of novel groupings not readily apparent in other clustering
801 methods. However, this method is resource intensive and with higher
802 dimensionality the number of genes that can be analyzed is limited. Because of
803 this, Barnes-Hut-SNE a newer implementation of *t*-SNE was used, which greatly
804 increases the speed and number of genes that can be analyzed (van der Maaten,
805 2013). It accomplishes this through the use of a Vantage Point tree and a variant
806 of the Barnes-Hut algorithm (van der Maaten, 2013). For clustering, 2D maps
807 were generated using a perplexity of 30 and without the initial PCA step from the
808 Barnes-Hut-SNE R implementation (Rtsne package; (Krijthe, 2014)). Theta was

809 set to 0.3 based on (van der Maaten, 2013) in order to maintain an accurate
810 dimensionality reduction without sacrificing processing speed.

811 **Clustering for Module Selection:** The DBscan algorithm (Density Based spatial
812 clustering of applications with noise) was used to select modules from the
813 Barnes-Hut-SNE results (fpc package; (Hennig, 2014)). This had the advantage
814 of both selecting modules and removing any genes that fell between modules.
815 The scanning range (*epsilon*) and minimum seed points (*minpts*) were selected
816 manually, and used to determine if any one point is a member of a cluster based
817 on physical positioning within the mapping relative to neighboring points.. A
818 *minpts* of 25 was used to capture smaller modules on the periphery and an
819 *epsilon* of 2.25 was used to avoid the overlapping of internal and closely spaced
820 modules.

821 **Plots:** Boxplots were generated from normalized expression values for each
822 module. The ribbon plot was generated from correlated expression values from
823 leaf development and photosynthesis related modules. These plots were
824 generated using ggplot from the ggplot2 R Package (Wickham, 2009). The
825 median expression of the genes mapped to a module was calculated for each IL
826 and replicated for all modules. Significant ILs were identified as those with a
827 median expression greater than 1 standard deviation from the mean of all genes
828 across all ILs in the module.

829

830 **GO Enrichment analysis**

831 Differentially expressed genes for individual ILs and Genes with significant eQTL
832 were analyzed for enrichment of Gene Ontology (GO) terms at a 0.05 false
833 discovery rate cutoff (goseq Bioconductor package; Young et al., 2010).

834

835 **Promoter enrichment analysis**

836 Promoter enrichment analysis was performed by analyzing the 1000 bp upstream
837 of the ATG translational start site for genes with significant eQTL using 100
838 motifs represented in the AGRIS AtTFDB ([http://arabidopsis.med.ohio-](http://arabidopsis.med.ohio-state.edu/AtTFDB)
839 [state.edu/AtTFDB](http://arabidopsis.med.ohio-state.edu/AtTFDB)). The Biostrings package was used to analyze the abundance
840 of 100 motifs in groups of genes with significant eQTL compared to motif
841 abundance in promoters of all analyzed genes using a Fisher's exact test ($p <$
842 0.05) with either zero or one mismatch (Ichihashi et al., 2014).

843

844 **Dissection of eQTL to different stages and time of development at shoot** 845 **apex**

846 Differentially expressed genes with enriched expression in laser micro-dissected
847 SAM/P0 vs. P1 samples or hand-dissected samples of the SAM + P0-P4 or P5
848 sampled over developmental time were obtained from Chitwood et al., 2015.
849 Genes for which a differential expression call could be made (i.e., had enough
850 reads and passed quality filters) were merged with detected eQTL using the
851 `merge()` function in R (R Core Team, 2015). For bootstrapping, *cis*- and *trans*-
852 regulated transcripts were analyzed separately. Merged gene expression
853 patterns were randomly permuted (without replacement) using the `sample()`

854 function against bin identity. For each test, 10,000 permutations were sampled to
855 count the times that a particular expression pattern was assigned to a bin more
856 than the actual count. Resulting frequencies, representing a probability value,
857 were multiple test adjusted using the Benjamini-Hochberg (Benjamini and
858 Hochberg, 1995) method using `p.adjust()`. Those bins with multiple test adjusted
859 probability values <0.05 were analyzed further using visualizations created with
860 `ggplot2` (Wickham, 2009).

861

862 **Sequence submission**

863 The quality filtered, barcode-sorted and trimmed short read dataset, which was
864 used to get the normalized read counts and for differential gene expression
865 analysis, was deposited to the NCBI Short Read Archive under accessions
866 SRR1013035 - SRR1013343 (Bioproject accession SRP031491).

867 **Supplemental files**

868

869 **Supplemental figures:**

870 **Supplemental Figure S1. Number of genes in the introgression region for**
871 **an IL and the number of differentially expressed genes compared to cv.**

872 **M82.** Strong correlation was observed for differentially expressed genes in *cis* (A),
873 whereas a weak correlation was observed for genes in *trans* (B).

874

875 **Supplemental Figure S2. Histograms for differentially expressed genes for**
876 **the ILs.** Up-regulated and down-regulated genes for the ILs in *cis* (A), and in
877 *trans* (B).

878

879 **Supplemental Figure S3. Frequency and distribution of differentially**
880 **expressed genes for the IL population at the introgression and the bin level.**

881 (A) Frequency of genes differentially expressed in one or more ILs. (B)
882 Frequency of genes being regulated by one or more BINs/eQTL. (C) Distribution
883 of genes under one or more eQTL regulation for the IL population on different
884 chromosomes

885

886 **Supplemental Figure S4. eQTL and the gene expression pattern they**
887 **regulate.** Each blue bar is a unique introgression. When the gene expression
888 pattern of gene 1 is correlated with bin-A, then bin-A contains a *cis*-eQTL. When
889 the gene expression pattern of gene 1 is correlated with bin-E then bin-E
890 contains a *trans*-eQTL. When gene 2 has a *cis*-eQTL designated for bin-D and
891 the gene expression pattern of gene 2 is also correlated with bin-B, then this
892 secondary correlation is not designated as an eQTL, since these bins share
893 overlapping introgression regions. When the gene expression pattern of gene 2
894 is correlated with bin-B and gene 2 does not have a *cis*-eQTL designated for bin-
895 D, then bin-B is designated as a *trans*-eQTL. All eQTLs for genes that lie in the
896 unassembled portion of the genome (not on any chromosome) cannot be
897 designated as either *cis*- or *trans*- and are designated *chromo0*-eQTL.

898

899 **Supplemental Figure S5. *Cis*- and *Trans*-eQTL.** Histograms plotting the
900 numbers of significant eQTL mapped to each bin across the 12 chromosomes of
901 *S. lycopersicum* (M82). A. *cis*-eQTLs. B. *trans*-eQTLs.

902

903 **Supplemental Figure S6. Boxplots of the normalized expression patterns**
904 **for the three landmark modules.** The relative expression of all genes found in
905 each module for the 74 IL's. The y-axis is the relative expression of all eQTL for
906 each IL. (A) Photosynthesis module. (B) Defense, metabolism, and signaling
907 module. (C) Cysteine-type peptidase activity module. Asterisks represent ILs with
908 a median expression significantly different from the module mean.

909

910 **Supplemental Figure S7. Normalized expression of the leaf development**
911 **module and leaf developmental genes within the mapping.** (A) Boxplot of
912 normalized expression pattern for the leaf development module. The 108 genes
913 contained in the leaf development module and their relative median expression
914 for each IL. Asterisks represent ILs with a median expression significantly
915 different from the module mean. (B) LC+ list of leaf developmental genes overlaid
916 on the Leaf Development and Photosynthesis modules. False colored orange,
917 dark blue, and light blue respectively.

918

919 **Supplemental Figure S8. eQTL regulation of gene expression patterns that**
920 **correlate with leaf number.**

921 A, B) Forty-two distinct modules identified by DBscan from the eQTL mapping
922 generated by BH-SNE analysis. Modules enriched for genes with leaf
923 development and photosynthesis GO terms are labeled in blue and green,
924 respectively. Genes with expression patterns correlated with leaf number under
925 simulated sun (A) and shade (B) are indicated by squares with positive
926 correlations in red and negative correlations in yellow.

927 C, D) Genes with expression patterns correlated with leaf number under
928 simulated sun (C) and shade (D) are shown connected to their respective eQTL
929 with chords. I) The 12 tomato chromosomes in megabases. II) Colored boxes
930 indicate the sizes of each bin. III) Black bars indicate the locations of the genes.
931 IV) Chords connect eQTL to the genes whose expression patterns they regulate.
932 Chords are colored by the chromosome location of the eQTL.

933

934 **Supplemental Figure S9. eQTL regulation of gene expression patterns that**
935 **correlate with leaf complexity.**

936 A, B) Forty-two distinct modules identified by DBscan from the eQTL mapping
937 generated by BH-SNE analysis. Modules enriched for genes with leaf
938 development and photosynthesis GO terms are labeled in blue and green,
939 respectively. Genes with expression patterns correlated with leaf complexity
940 under simulated sun (A) and shade (B) are indicated by squares with positive
941 correlations in red and negative correlations in yellow.

942 C, D) Genes with expression patterns correlated with leaf complexity under
943 simulated sun (C) and shade (D) are shown connected to their respective eQTL

944 with chords. I) The 12 tomato chromosomes in megabases. II) Colored boxes
945 indicate the sizes of each bin. III) Black bars indicate the locations of the genes.
946 IV) Chords connect eQTL to the genes whose expression patterns they regulate.
947 Chords are colored by the chromosome location of the eQTL.

948

949 **Supplemental Figure S10. Distributions of introgressions from *S. pennellii***
950 **into *S. lycopersicum* cv. M82.** Map of chromosomes 2, 10, and 11 showing the
951 locations of the introgressions for BIL 033 and 128, as well as the overlapping IL
952 regions, which define the bind (Modified from Chitwood et al., 2013).

953

954 **Supplemental Figure S11. Tomato hypocotyl length under sun and shade**
955 **treatments.** M82 shows a typical shade response with a significantly longer
956 hypocotyl in the shade (Δ of 7 mm). IL 10.1 and BIL 128, which share an
957 overlapping introgression (**Supplemental Fig. BIL**), do not significantly respond
958 to the shade treatments. The presence of a response in BIL 033 in combination
959 with the shared introgression with BIL 128 on chromosome 2, indicates that the
960 gene region responsible for the lack of shade response in BIL 128 is located in
961 the introgression on chromosome 10. Bars represent means \pm SE with a
962 minimal of $N = 22$ for each (ANOVA, $F_{7,182} = 44.6$, $p < 0.001$). Letters indicate
963 differences at the $p < 0.05$ significance level for Tukey pairwise tests.

964

965 **Supplemental Figure S12. Quantification of genes with transgressive**
966 **expression pattern in the IL population (A) Number of genes showing**

967 transgressive expression for each IL along with their location in *cis* or *trans*. (B)
968 Ratio of number of genes with transgressive expression to number of genes with
969 *S. pennellii* like expression (transgressive to *S. pennellii*-like) for each IL.

970

971 **Supplemental tables:**

972 **Supplemental Table I. Number of differentially expressed (DE) genes in *cis*,**
973 ***trans*, and the total number of DE genes for the ILs along with number of**
974 **genes in the introgression region.**

975

976 **Supplemental Table II. Correlation coefficients (Spearman's rho) for**
977 **significant eQTLs.** Divided into *trans*-, *cis*-, and *chromo0*-, then designated as
978 up (positive slope) or down (negative slope) based on the correlation coefficients.

979

980 **Supplemental Table III. GO enrichment and *cis* or *trans* regulation of the 42**
981 **identified modules.** All 42 distinct modules are listed with the total number of
982 genes present in each module. The GO enrichment (if one is present) is given
983 for each module, along with whether that module is predominantly *cis* or *trans*
984 regulated. Only nine of the forty two module show *trans* correlation, which
985 includes the leaf development module.

986

987 **Supplemental Table IV. Significant correlations between gene expression**
988 **patterns and phenotypes.** Bootstrapping analyses correlated gene expression

989 patterns across the 74 ILs with three phenotypes in under both sun and shade
990 treatments. Genes with significant correlations that also have eQTL are listed.

991

992 **Supplemental datasets:**

993 **Supplemental Dataset 1. List of Differentially Expressed Genes.** List of
994 significant (FDR < 0.05) differentially expressed genes for each Introgression line
995 (IL) compared to cultivated parent *Solanum lycopersicum* cv. M82. For each IL,
996 gene ID, log Fold Change (logFC), log Counts Per Million (logCPM), P-value,
997 False Discovery Rate (FDR) as well as annotation of the differentially expressed
998 genes are presented.

999

1000 **Supplemental Dataset 2. Frequency of differentially expressed genes**
1001 **among the ILs** (Genes that show differential expression in at least one IL are
1002 listed).

1003 **Supplemental Dataset 3. All eQTL.** All significant eQTL with AGI and ITAG
1004 annotations added.

1005 **Supplemental Dataset 4. Number of eQTL per bin.**

1006

1007 **Supplemental Dataset 5. Number of eQTL and the bin on which they reside**
1008 **for each of the landmark modules.** The Photosynthesis, Defense and
1009 Cysteine-Type Peptidase Activity modules are listed with the bins on which their
1010 eQTL reside. The number eQTL per bin and the percentage of total eQTL within
1011 each module is listed.

1012

1013 **Supplemental Dataset 6. Module Gene List.** Listing of all genes within the
1014 Photosynthesis module with Gene ID and Description.

1015

1016 **Supplemental Dataset 7. Module Gene List.** Listing of all genes within the
1017 Defense module with Gene ID and Description.

1018

1019 **Supplemental Dataset 8. Module Gene List.** Listing of all genes within the
1020 Cysteine-type Peptidase module with Gene ID and Description.

1021

1022 **Supplemental Dataset 9. GO Enrichment for DE Genes.** Enriched GO and
1023 GOslim categories for the up- and down-regulated genes in each IL compared to
1024 cultivated parent *Solanum lycopersicum* cv. M82.

1025

1026 **Supplemental Dataset 10. GO Enrichment for eQTL.** GO and GO SLIM
1027 enrichment results for all the eQTL mapped to a bin, as well as the *cis*- and
1028 *trans*-eQTL separately.

1029

1030 **Supplemental Dataset 11. Promoter Motif Enrichment for DE Genes.**
1031 Enriched promoter motifs with no mismatch for the up- and down-regulated
1032 genes in each IL compared to cultivated parent *Solanum lycopersicum* cv. M82.

1033

1034 **Supplemental Dataset 12. Enriched promoter motifs for *trans*-eQTLs**

1035 **mapped to each bin.**

1036

1037 **Supplemental Dataset 13. Differentially expressed leaf Developmental**

1038 **Genes.** Frequency of differentially expressed literature-curated leaf-

1039 developmental genes among the ILs (Genes that show differential expression in

1040 at least one IL are listed).

1041

1042 **Supplemental Dataset 14. Curated list of leaf developmental genes with**

1043 **eQTLs.**

1044

1045 **Supplemental Dataset 15. Literature-curated plus list of leaf development**

1046 **genes present in the leaf development modules.** Nineteen genes from the

1047 literature-curated plus list (Ichihashi et al., 2014) were present within the leaf

1048 development module, representing approximately 3% of the curated genes and

1049 11% of the curated genes found in the eQTL data set. The Gene ID, *Arabidopsis*

1050 orthologue, and a description for each gene is provided.

1051

1052 **Supplemental Dataset 16. Literature-curated plus list of leaf development**

1053 **genes that are present in all modules.** A total of 175 genes from the curated

1054 list plus of leaf developmental genes (Ichihashi et al., 2014) were present in the

1055 5289 genes with significant eQTL. Matching gene number is the number of

1056 genes in the module, which were found in the curated list. The percent of curated

1057 genes defines the percentage of matched genes in a module out of the total
1058 curated list plus. The percent total in eQTL represents the percentage of
1059 matched genes in a module out of the 175 present only in the eQTL. The
1060 Photosynthesis and leaf development modules contain the highest proportion of
1061 leaf development curated genes.

1062

1063 **Supplemental Dataset 17. Module Gene List.** Listing of all genes within the
1064 Leaf Development module with Gene ID and Description.

1065

1066 **Supplemental Dataset 18: GO enrichment results for bins statically**
1067 **enriched for genes expressed spatio-temporally across tissues.**

1068

1069 **Supplemental Dataset 19: Total leaf complexity data for all the ILs under**
1070 **simulated sun and shade.**

1071

1072 **Supplemental Dataset 20: Hypocotyl length data for all the ILs under**
1073 **simulated sun and shade for two years.**

1074

1075 **Supplemental Dataset 21. Genes with Transgressive Expression.** List of the
1076 genes showing transgressive expression in the IL population along with details of
1077 their expression and annotation.

1078

1079 **Supplemental Dataset 22. GO Enrichment for Transgressive Expression.**

1080 Enriched GO-categories for the genes showing transgressive expression in the IL
1081 population.

1082

1083 **Acknowledgments**

1084 We thank Lauren R. Headland, Jason Kao and Paradee Thammaphichai for help
1085 in generating plant materials. We also thank Mike Covington for his advice on
1086 bioinformatic analyses. We thank the Vincent J. Coates Genomics Sequencing
1087 Laboratory at UC Berkeley (supported by NIH S10 Instrumentation Grants
1088 S10RR029668 and S10RR027303), and computational resources/cyber
1089 infrastructure provided by the iPlant Collaborative (www.iplantcollaborative.org),
1090 funded by the National Science Foundation (Grant DBI-0735191).

1091

1092 **Authors' contributions**

1093 DHC, JNM and NRS conceived and designed the experiments. AR, DHC, RK,
1094 LC, YI and KZ performed the experiments. AR, JMB and SDR analyzed the data.
1095 AR, JMB, SDR, DHC and JNM contributed reagents/materials/analysis tools. AR,
1096 JMB, SDR and NRS wrote the paper. All authors read and approved the final
1097 manuscript.

1098

1099

1100 **Figure legends:**

1101 **Figure 1. Transcriptome profile of the tomato introgression lines.**

1102 Differentially expressed genes for the ILs compared to cultivated parent M82. Y-
1103 axis shows all the tomato genes starting from the first gene on chromosome 1 to
1104 the last gene on chromosome 12, and X-axis depicts the individual ILs. Genes
1105 differentially expressed within the introgression regions (in *cis*) are shown as blue
1106 points and differentially expressed genes in *trans* (outside) the introgression
1107 region are shown as orange points.

1108

1109 **Figure 2. *Cis*- and *Trans*-eQTL plotted by bin across the 12 chromosomes**

1110 **of *S. lycopersicum* cv. M82.** A) Stacked bar graph showing the sum of the
1111 number of eQTL mapping to each bin. B) Dotplot showing each eQTL arranged
1112 vertically by bin and horizontally by the location of the gene expression pattern it
1113 regulates. Bins with the largest numbers of *trans*-eQTL (4D, 4E, 4F, 6B, 6C, 8A,
1114 8B) are highlighted by green boxes. C) Map of chromosomes 4, 6, and 8 showing
1115 the overlapping IL regions, which define the bins (Modified from Chitwood et al.,
1116 2013). Bins with the largest numbers of *trans*-eQTL are indicated by green
1117 asterisks.

1118

1119 **Figure 3. BH-SNE 2D mapping of eQTL.** (A) Forty-two distinct modules

1120 identified by DBscan from the mapping generated by BH-SNE analysis. (B) The

1121 three modules defined as landmark modules: photosynthesis, defense and

1122 cysteine-type peptidase activity and the leaf development module's position
1123 within the mapping. Modules are false colored.

1124

1125 **Figure 4. Connections between eQTL and the genes they regulate.** Each plot
1126 includes the genes with eQTL that were clustered together into a module based
1127 on expression patterns. A) Defense module. B) Photosynthesis module. C)
1128 Cysteine peptidase module. D) Leaf development module. I) The 12 tomato
1129 chromosomes in megabases. II) Colored boxes indicate the sizes of each bin. III)
1130 Black bars indicate the locations of the genes. IV) Chords connect eQTL to the
1131 genes whose expression patterns they regulate. Chords are colored by the
1132 chromosome location of the eQTL.

1133

1134 **Figure 5. Median expression values for leaf development and**
1135 **photosynthesis related modules and expression correlation.** (A) The
1136 median expression values of a module for each IL are shown. A consistent
1137 negative correlation between photosynthesis and Leaf development transcript
1138 expression is evident across nearly all 74 ILs. Dashed lines indicate one
1139 significant deviation from the module mean expression. Filled areas represent
1140 the median expression of the leaf development module, while open areas
1141 indicate the photosynthesis module median expression. (B) Leaf development
1142 median expression versus photosynthesis median expression values for each IL
1143 show a distinct negative correlation with an adjusted R-squared value of 0.77
1144 (calculated by linear regression in R).

1145

1146 **Figure 6. Enriched expression patterns for genes genetically regulated by**

1147 **bins. A)** Log fold change values (P1/SAM+P0) for previously identified

1148 differentially expressed genes with high expression in the SAM + P0 (magenta)

1149 vs. P1 (green). **B)** Scaled gene expression values for previously identified

1150 differentially expressed genes with increasing (red) and decreasing (blue)

1151 expression over developmental time in the SAM + P0-P4. **C)** Scaled gene

1152 expression values for previously identified differentially expressed genes with

1153 increasing (orange) and decreasing (purple) expression over developmental time

1154 in P5. **D)** Transcripts (y-axis) and bins (x-axis) showing the genetic regulation of

1155 gene expression (eQTL). Colors indicate SAM + P0 (magenta) and P1 (green)

1156 transcripts. Bins enriched for genetically regulating genes with specific

1157 expression patterns are indicated below with triangles. **E)** Same as in D), except

1158 showing genes with increasing (red) and decreasing (blue) expression over

1159 temporal time in the SAM + P0-P4. **F)** Same as in D), except showing genes with

1160 increasing (orange) and decreasing (purple) expression over temporal time in P5.

1161 Previously determined gene expression patterns are previously published

1162 (Chitwood et al., 2015).

1163

1164 **Figure 7. eQTL regulation of gene expression patterns that correlate with**

1165 **hypocotyl length.**

1166 A) Forty-two distinct modules identified by DBscan from the eQTL mapping

1167 generated by BH-SNE analysis. Modules enriched for genes with leaf

1168 development and photosynthesis GO terms are labeled in blue and green,
1169 respectively. Genes with expression patterns correlated with hypocotyl length
1170 under simulated shade are indicated by squares with positive correlations in red
1171 and negative correlations in yellow.

1172 B) Genes with expression patterns correlated with hypocotyl length under
1173 simulated shade are shown connected to their respective eQTL with chords. I)
1174 The 12 tomato chromosomes in megabases. II) Colored boxes indicate the sizes
1175 of each bin. III) Black bars indicate the locations of the genes. IV) Chords
1176 connect eQTL to the genes whose expression patterns they regulate. Chords are
1177 colored by the chromosome location of the eQTL.

1178

1179

Parsed Citations

bioRxiv preprint first posted online Feb 22, 2016. doi: <https://doi.org/10.1101/040592>. The copyright holder for this preprint (which was not certified by peer review) is the author/funder. All rights reserved. No reuse allowed without permission.

Abe M, Katsumata H, Komeda Y, Takahashi F (2003) Regulation of shoot epidermal cell differentiation by a pair of homeodomain proteins in Arabidopsis. Development 130: 635-643
Pubmed: [Author and Title](#)
CrossRef: [Author and Title](#)
Google Scholar: [Author Only](#) [Title Only](#) [Author and Title](#)

Abramoff MD, Magalhaes PJ, Ram SJ (2004) Image Processing with ImageJ. Biophotonics International 11: 36-42
Pubmed: [Author and Title](#)
CrossRef: [Author and Title](#)
Google Scholar: [Author Only](#) [Title Only](#) [Author and Title](#)

Battle A, Khan Z, Wang SH, Mitrano A, Ford MJ, Pritchard JK, Gilad Y (2015) Genomic variation. Impact of regulatory variation from RNA to protein. Science 347: 664-667
Pubmed: [Author and Title](#)
CrossRef: [Author and Title](#)
Google Scholar: [Author Only](#) [Title Only](#) [Author and Title](#)

Benjamini Y, Hochberg Y (1995) Controlling the false discovery rate: A practical and powerful approach to multiple testing. J R Stat Soc B 57: 289-300
Pubmed: [Author and Title](#)
CrossRef: [Author and Title](#)
Google Scholar: [Author Only](#) [Title Only](#) [Author and Title](#)

Brem RB, Kruglyak L (2005) The landscape of genetic complexity across 5,700 gene expression traits in yeast. Proc Natl Acad Sci U S A 102: 1572-1577
Pubmed: [Author and Title](#)
CrossRef: [Author and Title](#)
Google Scholar: [Author Only](#) [Title Only](#) [Author and Title](#)

Brem RB, Yvert G, Clinton R, Kruglyak L (2002) Genetic dissection of transcriptional regulation in budding yeast. Science 296: 752-755
Pubmed: [Author and Title](#)
CrossRef: [Author and Title](#)
Google Scholar: [Author Only](#) [Title Only](#) [Author and Title](#)

Bushati N, Smith J, Briscoe J, Watkins C (2011) An intuitive graphical visualization technique for the interrogation of transcriptome data. Nucleic Acids Res 39: 7380-7389
Pubmed: [Author and Title](#)
CrossRef: [Author and Title](#)
Google Scholar: [Author Only](#) [Title Only](#) [Author and Title](#)

Carles CC, Choffnes-Inada D, Reville K, Lertpiriyapong K, Fletcher JC (2005) ULTRAPETALA1 encodes a SAND domain putative transcriptional regulator that controls shoot and floral meristem activity in Arabidopsis. Development 132: 897-911
Pubmed: [Author and Title](#)
CrossRef: [Author and Title](#)
Google Scholar: [Author Only](#) [Title Only](#) [Author and Title](#)

Chen X, Hackett CA, Nicks RE, Hedley PE, Booth C, Druka A, Marcel TC, Vels A, Bayer M, Milne I, Morris J, Ramsay L, Marshall D, Cardle L, Waugh R (2010) An eQTL analysis of partial resistance to Puccinia hordei in barley. PLoS One 5: e8598
Pubmed: [Author and Title](#)
CrossRef: [Author and Title](#)
Google Scholar: [Author Only](#) [Title Only](#) [Author and Title](#)

Chitwood DH, Kumar R, Headland LR, Ranjan A, Covington MF, Ichihashi Y, Fulop D, Jimenez-Gomez JM, Peng J, Maloof JN, Sinha NR (2013) A quantitative genetic basis for leaf morphology in a set of precisely defined tomato introgression lines. Plant Cell 25: 2465-2481
Pubmed: [Author and Title](#)
CrossRef: [Author and Title](#)
Google Scholar: [Author Only](#) [Title Only](#) [Author and Title](#)

Chitwood DH, Kumar R, Ranjan A, Pelletier JM, Townsley BT, Ichihashi Y, Martinez CC, Zumstein K, Harada JJ, Maloof JN, Sinha NR (2015) Light-Induced Indeterminacy Alters Shade-Avoiding Tomato Leaf Morphology. Plant Physiol 169: 2030-2047
Pubmed: [Author and Title](#)
CrossRef: [Author and Title](#)
Google Scholar: [Author Only](#) [Title Only](#) [Author and Title](#)

Chitwood DH, Ranjan A, Kumar R, Ichihashi Y, Zumstein K, Headland LR, Ostria-Gallardo E, Aguilar-Martinez JA, Bush S, Carriedo L, Fulop D, Martinez CC, Peng J, Maloof JN, Sinha NR (2014) Resolving distinct genetic regulators of tomato leaf shape within a heteroblastic and ontogenetic context. Plant Cell 26: 3616-3629
Pubmed: [Author and Title](#)
CrossRef: [Author and Title](#)
Google Scholar: [Author Only](#) [Title Only](#) [Author and Title](#)

Chitwood DH, Sinha NR (2013) A census of cells in time: quantitative genetics meets developmental biology. Curr Opin Plant Biol 16: 92-99
Pubmed: [Author and Title](#)
CrossRef: [Author and Title](#)

Google Scholar: [Author Only](#) [Title Only](#) [Author and Title](#)

Clark RM, Wagler TN, Quijada P, Doebley J (2006) A distant upstream enhancer at the maize domestication gene tb1 has pleiotropic effects on plant and inflorescent architecture. Nat Genet 38: 594-597

Pubmed: [Author and Title](#)

CrossRef: [Author and Title](#)

Google Scholar: [Author Only](#) [Title Only](#) [Author and Title](#)

Cnops G, Jover-Gil S, Peters JL, Neyt P, De Block S, Robles P, Ponce MR, Gerats T, Micol JL, Van Lijsebettens M (2004) The rotunda2 mutants identify a role for the LEUNIG gene in vegetative leaf morphogenesis. J Exp Bot 55: 1529-1539

Pubmed: [Author and Title](#)

CrossRef: [Author and Title](#)

Google Scholar: [Author Only](#) [Title Only](#) [Author and Title](#)

Cubillos FA, Coustham V, Loudet O (2012) Lessons from eQTL mapping studies: non-coding regions and their role behind natural phenotypic variation in plants. Curr Opin Plant Biol 15: 192-198

Pubmed: [Author and Title](#)

CrossRef: [Author and Title](#)

Google Scholar: [Author Only](#) [Title Only](#) [Author and Title](#)

Cubillos FA, Yansouni J, Khalili H, Balzergue S, Elftieh S, Martin-Magniette ML, Serrand Y, Lepiniec L, Baud S, Dubreucq B, Renou JP, Camilleri C, Loudet O (2012) Expression variation in connected recombinant populations of Arabidopsis thaliana highlights distinct transcriptome architectures. BMC Genomics 13: 117

Pubmed: [Author and Title](#)

CrossRef: [Author and Title](#)

Google Scholar: [Author Only](#) [Title Only](#) [Author and Title](#)

DeCook R, Lall S, Nettleton D, Howell SH (2006) Genetic regulation of gene expression during shoot development in Arabidopsis. Genetics 172: 1155-1164

Pubmed: [Author and Title](#)

CrossRef: [Author and Title](#)

Google Scholar: [Author Only](#) [Title Only](#) [Author and Title](#)

Diaz-Mendoza M, Velasco-Arroyo B, Gonzalez-Melendi P, Martinez M, Diaz I (2014) C1A cysteine protease-cystatin interactions in leaf senescence. J Exp Bot 65: 3825-3833

Pubmed: [Author and Title](#)

CrossRef: [Author and Title](#)

Google Scholar: [Author Only](#) [Title Only](#) [Author and Title](#)

Druka A, Potokina E, Luo Z, Jiang N, Chen X, Kearsley M, Waugh R (2010) Expression quantitative trait loci analysis in plants. Plant Biotechnol J 8: 10-27

Pubmed: [Author and Title](#)

CrossRef: [Author and Title](#)

Google Scholar: [Author Only](#) [Title Only](#) [Author and Title](#)

Eshed Y, Zamir D (1995) An introgression line population of Lycopersicon pennellii in the cultivated tomato enables the identification and fine mapping of yield-associated QTL. Genetics 141: 1147-1162

Pubmed: [Author and Title](#)

CrossRef: [Author and Title](#)

Google Scholar: [Author Only](#) [Title Only](#) [Author and Title](#)

Frary A, Nesbitt TC, Grandillo S, Knaap E, Cong B, Liu J, Meller J, Elber R, Alpert KB, Tanksley SD (2000) fw2.2: a quantitative trait locus key to the evolution of tomato fruit size. Science 289: 85-88

Pubmed: [Author and Title](#)

CrossRef: [Author and Title](#)

Google Scholar: [Author Only](#) [Title Only](#) [Author and Title](#)

Fridman E, Carrari F, Liu YS, Fernie AR, Zamir D (2004) Zooming in on a quantitative trait for tomato yield using interspecific introgressions. Science 305: 1786-1789

Pubmed: [Author and Title](#)

CrossRef: [Author and Title](#)

Google Scholar: [Author Only](#) [Title Only](#) [Author and Title](#)

Fukao T, Xu K, Ronald PC, Bailey-Serres J (2006) A variable cluster of ethylene response factor-like genes regulates metabolic and developmental acclimation responses to submergence in rice. Plant Cell 18: 2021-2034

Pubmed: [Author and Title](#)

CrossRef: [Author and Title](#)

Google Scholar: [Author Only](#) [Title Only](#) [Author and Title](#)

Fulop D, Ranjan A, Ofner I, Covington MF, Chitwood DH, West D, Ichihashi Y, Headland L, Zamir D, Maloof JN, Sinha NR A new advanced backcross tomato population enables high resolution leaf QTL mapping and gene identification. Plant Physiology Int Review.

Goff SA, Vaughn M, McKay S, Lyons E, Stapleton AE, Gessler D, Matasci N, Wang L, Hanlon M, Lenards A, Muir A, Merchant N, Lowry S, Mock S, Helmke M, Kubach A, Narro M, Hopkins N, Micklos D, Hilgert U, Gonzales M, Jordan C, Skidmore E, Dooley R, Cazes J, McLay R, Lu Z, Pasternak S, Koesterke L, Piel WH, Grene R, Noutsos C, Gendler K, Feng X, Tang C, Lent M, Kim SJ, Kvilekval K, Manjunath BS, Tannen V, Stamatakis A, Sanderson M, Welch SM, Cranston KA, Soltis P, Soltis D, O'Meara B, Ane C, Brutnell T, Kleibenstein DJ, White JW, Leebens-Mack J, Donoghue MJ, Spalding EP, Vision TJ, Myers CR, Lowenthal D, Enquist BJ, Boyle B, Akoglu A, Andrews G, Ram S, Ware D, Stein L, Stanzione D (2011) The iPlant Collaborative: Cyberinfrastructure for Plant Biology. Front Plant Sci 2: 34

Pubmed: [Author and Title](#)

CrossRef: [Author and Title](#)

Google Scholar: [Author Only Title Only Author and Title](#)

bioRxiv preprint first posted online Feb. 22, 2016; doi: <http://dx.doi.org/10.1101/040592>. The copyright holder for this preprint (which was not certified by peer review) is the author/funder, who has granted bioRxiv a license to display the preprint in perpetuity. It is made available under aCC-BY-NC-ND 4.0 International license.

Hammond JP, Mayes S, Bowen PC, Graffius S, Hayden RM, Love CG, Spradler WP, Wang U, Williams S, White PJ, King GJ, Broadley MR (2011) Regulatory hotspots are associated with plant gene expression under varying soil phosphorus supply in *Brassica rapa*. *Plant Physiol* 156: 1230-1241

Pubmed: [Author and Title](#)

CrossRef: [Author and Title](#)

Google Scholar: [Author Only Title Only Author and Title](#)

Hegarty MJ, Barker GL, Brennan AC, Edwards KJ, Abbott RJ, Hiscock SJ (2008) Changes to gene expression associated with hybrid speciation in plants: further insights from transcriptomic studies in *Senecio*. *Philos Trans R Soc Lond B Biol Sci* 363: 3055-3069

Pubmed: [Author and Title](#)

CrossRef: [Author and Title](#)

Google Scholar: [Author Only Title Only Author and Title](#)

Hennig C (2014) FPC: Flexible procedures for Clustering. R Package Version: 2.1-9

Pubmed: [Author and Title](#)

CrossRef: [Author and Title](#)

Google Scholar: [Author Only Title Only Author and Title](#)

Holloway B, Li B (2010) Expression QTLs: applications for crop improvement. *Molecular Breeding* 26: 381-391

Pubmed: [Author and Title](#)

CrossRef: [Author and Title](#)

Google Scholar: [Author Only Title Only Author and Title](#)

Holloway B, Luck S, Beatty M, Rafalski JA, Li B (2011) Genome-wide expression quantitative trait loci (eQTL) analysis in maize. *BMC Genomics* 12: 336

Pubmed: [Author and Title](#)

CrossRef: [Author and Title](#)

Google Scholar: [Author Only Title Only Author and Title](#)

Holtan HE, Hake S (2003) Quantitative trait locus analysis of leaf dissection in tomato using *Lycopersicon pennellii* segmental introgression lines. *Genetics* 165: 1541-1550

Pubmed: [Author and Title](#)

CrossRef: [Author and Title](#)

Google Scholar: [Author Only Title Only Author and Title](#)

Ichihashi Y, Aguilar-Martinez JA, Farhi M, Chitwood DH, Kumar R, Millon LV, Peng J, Maloof JN, Sinha NR (2014) Evolutionary developmental transcriptomics reveals a gene network module regulating interspecific diversity in plant leaf shape. *Proc Natl Acad Sci U S A* 111: E2616-2621

Pubmed: [Author and Title](#)

CrossRef: [Author and Title](#)

Google Scholar: [Author Only Title Only Author and Title](#)

Jansen RC, Nap JP (2001) Genetical genomics: the added value from segregation. *Trends Genet* 17: 388-391

Pubmed: [Author and Title](#)

CrossRef: [Author and Title](#)

Google Scholar: [Author Only Title Only Author and Title](#)

Keurentjes JJ, Fu J, Terpstra IR, Garcia JM, van den Ackerveken G, Snoek LB, Peeters AJ, Vreugdenhil D, Koornneef M, Jansen RC (2007) Regulatory network construction in *Arabidopsis* by using genome-wide gene expression quantitative trait loci. *Proc Natl Acad Sci U S A* 104: 1708-1713

Pubmed: [Author and Title](#)

CrossRef: [Author and Title](#)

Google Scholar: [Author Only Title Only Author and Title](#)

Kliebenstein D (2009) Quantitative genomics: analyzing intraspecific variation using global gene expression polymorphisms or eQTLs. *Annu Rev Plant Biol* 60: 93-114

Pubmed: [Author and Title](#)

CrossRef: [Author and Title](#)

Google Scholar: [Author Only Title Only Author and Title](#)

Kliebenstein DJ, West MA, van Leeuwen H, Kim K, Doerge RW, Michelmore RW, St Clair DA (2006) Genomic survey of gene expression diversity in *Arabidopsis thaliana*. *Genetics* 172: 1179-1189

Pubmed: [Author and Title](#)

CrossRef: [Author and Title](#)

Google Scholar: [Author Only Title Only Author and Title](#)

Koenig D, Jimenez-Gomez JM, Kimura S, Fulop D, Chitwood DH, Headland LR, Kumar R, Covington MF, Devisetty UK, Tat AV, Tohge T, Bolger A, Schneeberger K, Ossowski S, Lanz C, Xiong G, Taylor-Teeple M, Brady SM, Pauly M, Weigel D, Usadel B, Fernie AR, Peng J, Sinha NR, Maloof JN (2013) Comparative transcriptomics reveals patterns of selection in domesticated and wild tomato. *Proc Natl Acad Sci U S A* 110: E2655-2662

Pubmed: [Author and Title](#)

CrossRef: [Author and Title](#)

Google Scholar: [Author Only Title Only Author and Title](#)

Krijthe J (2014) Rtsne: T-distributed Stochastic Neighbor Embedding using Barnes-Hut implementation. R Package Version: 0.9

Pubmed: [Author and Title](#)

CrossRef: [Author and Title](#)

Google Scholar: [Author Only Title Only Author and Title](#)

bioRxiv preprint first posted online Feb. 22, 2016; doi: <http://dx.doi.org/10.1101/040592>. The copyright holder for this preprint (which was not certified by peer review) is the author/funder. All rights reserved. No reuse allowed without permission.

Kroymann J, Donnerhacke S, Schmalzer A, Mitchell-Olds KE (2009) Evolutionary dynamics of an Arabidopsis insect resistance quantitative trait locus. Proc Natl Acad Sci U S A 100 Suppl 2: 14587-14592

Pubmed: [Author and Title](#)

CrossRef: [Author and Title](#)

Google Scholar: [Author Only Title Only Author and Title](#)

Kumar R, Ichihashi Y, Kimura S, Chitwood DH, Headland LR, Peng J, Maloof JN, Sinha NR (2012) A High-Throughput Method for Illumina RNA-Seq Library Preparation. Front Plant Sci 3: 202

Pubmed: [Author and Title](#)

CrossRef: [Author and Title](#)

Google Scholar: [Author Only Title Only Author and Title](#)

Li H, Durbin R (2009) Fast and accurate short read alignment with Burrows-Wheeler transform. Bioinformatics 25: 1754-1760

Pubmed: [Author and Title](#)

CrossRef: [Author and Title](#)

Google Scholar: [Author Only Title Only Author and Title](#)

Liu YS, Zamir D (1999) Second generation *L. pennellii* introgression lines and the concept of bin mapping. Tomato Genet. Coop. Rep. 49: 26-30

Pubmed: [Author and Title](#)

CrossRef: [Author and Title](#)

Google Scholar: [Author Only Title Only Author and Title](#)

Longair MH, Baker DA, Armstrong JD (2011) Simple Neurite Tracer: open source software for reconstruction, visualization and analysis of neuronal processes. Bioinformatics 27: 2453-2454

Pubmed: [Author and Title](#)

CrossRef: [Author and Title](#)

Google Scholar: [Author Only Title Only Author and Title](#)

Moyle LC (2008) Ecological and evolutionary genomics in the wild tomatoes (*Solanum* sect. *Lycopersicon*). Evolution 62: 2995-3013

Pubmed: [Author and Title](#)

CrossRef: [Author and Title](#)

Google Scholar: [Author Only Title Only Author and Title](#)

Muir CD, Pease JB, Moyle LC (2014) Quantitative genetic analysis indicates natural selection on leaf phenotypes across wild tomato species (*Solanum* sect. *Lycopersicon*; *Solanaceae*). Genetics 198: 1629-1643

Pubmed: [Author and Title](#)

CrossRef: [Author and Title](#)

Google Scholar: [Author Only Title Only Author and Title](#)

Muller NA, Wijnen CL, Srinivasan A, Ryngajlo M, Ofner I, Lin T, Ranjan A, West D, Maloof JN, Sinha NR, Huang S, Zamir D, Jimenez-Gomez JM (2016) Domestication selected for deceleration of the circadian clock in cultivated tomato. Nat Genet 48: 89-93

Pubmed: [Author and Title](#)

CrossRef: [Author and Title](#)

Google Scholar: [Author Only Title Only Author and Title](#)

Pickrell JK, Marioni JC, Pai AA, Degner JF, Engelhardt BE, Nkadori E, Veyrieras JB, Stephens M, Gilad Y, Pritchard JK (2010) Understanding mechanisms underlying human gene expression variation with RNA sequencing. Nature 464: 768-772

Pubmed: [Author and Title](#)

CrossRef: [Author and Title](#)

Google Scholar: [Author Only Title Only Author and Title](#)

R Development CoreTeam (2015) R: A Language and Environment for Statistical Computing. (Vienna, Austria: R Foundation for Statistical Computing)

Pubmed: [Author and Title](#)

CrossRef: [Author and Title](#)

Google Scholar: [Author Only Title Only Author and Title](#)

Ranjan A, Ichihashi Y, Sinha NR (2012) The tomato genome: implications for plant breeding, genomics and evolution. Genome Biol 13: 167

Pubmed: [Author and Title](#)

CrossRef: [Author and Title](#)

Google Scholar: [Author Only Title Only Author and Title](#)

Riddle NC, Birchler JA (2003) Effects of reunited diverged regulatory hierarchies in allopolyploids and species hybrids. Trends Genet 19: 597-600

Pubmed: [Author and Title](#)

CrossRef: [Author and Title](#)

Google Scholar: [Author Only Title Only Author and Title](#)

Rieseberg LH, Archer MA, Wayne RK (1999) Transgressive segregation, adaptation and speciation. Heredity (Edinb) 83 (Pt 4): 363-372

Pubmed: [Author and Title](#)

CrossRef: [Author and Title](#)

Google Scholar: [Author Only Title Only Author and Title](#)

Roberts A, Pachter L (2013) Streaming fragment assignment for real-time analysis of sequencing experiments. Nat Methods 10: 71-

Pubmed: [Author and Title](#)

CrossRef: [Author and Title](#)

bioRxiv preprint first posted online Feb. 22, 2016; doi: <http://dx.doi.org/10.1101/040592>. The copyright holder for this preprint (which was not peer-reviewed) is the author/funder. All rights reserved. No reuse allowed without permission.

Robinson MD, Oshlack A (2010) A scaling normalization method for differential expression analysis of RNA-seq data. Genome Biol 11: R25

Pubmed: [Author and Title](#)

CrossRef: [Author and Title](#)

Google Scholar: [Author Only](#) [Title Only](#) [Author and Title](#)

Schadt EE, Molony C, Chudin E, Hao K, Yang X, Lum PY, Kasarskis A, Zhang B, Wang S, Suver C, Zhu J, Millstein J, Sieberts S, Lamb J, GuhaThakurta D, Derry J, Storey JD, Avila-Campillo I, Kruger MJ, Johnson JM, Rohl CA, van Nas A, Mehrabian M, Drake TA, Lusk AJ, Smith RC, Guengerich FP, Strom SC, Schuetz E, Rushmore TH, Ulrich R (2008) Mapping the genetic architecture of gene expression in human liver. PLoS Biol 6: e107

Pubmed: [Author and Title](#)

CrossRef: [Author and Title](#)

Google Scholar: [Author Only](#) [Title Only](#) [Author and Title](#)

Schadt EE, Monks SA, Drake TA, Lusk AJ, Che N, Colinayo V, Ruff TG, Milligan SB, Lamb JR, Cavet G, Linsley PS, Mao M, Stoughton RB, Friend SH (2003) Genetics of gene expression surveyed in maize, mouse and man. Nature 422: 297-302

Pubmed: [Author and Title](#)

CrossRef: [Author and Title](#)

Google Scholar: [Author Only](#) [Title Only](#) [Author and Title](#)

Sharlach M, Dahlbeck D, Liu L, Chiu J, Jimenez-Gomez JM, Kimura S, Koenig D, Maloof JN, Sinha N, Minsavage GV, Jones JB, Stall RE, Staskawicz BJ (2013) Fine genetic mapping of RXopJ4, a bacterial spot disease resistance locus from Solanum pennellii LA716. Theor Appl Genet 126: 601-609

Pubmed: [Author and Title](#)

CrossRef: [Author and Title](#)

Google Scholar: [Author Only](#) [Title Only](#) [Author and Title](#)

Shivaprasad PV, Dunn RM, Santos BA, Bassett A, Baulcombe DC (2012) Extraordinary transgressive phenotypes of hybrid tomato are influenced by epigenetics and small silencing RNAs. EMBO J 31: 257-266

Pubmed: [Author and Title](#)

CrossRef: [Author and Title](#)

Google Scholar: [Author Only](#) [Title Only](#) [Author and Title](#)

Svistonoff S, Creff A, Reymond M, Sigoillot-Claude C, Ricaud L, Blanchet A, Nussaume L, Desnos T (2007) Root tip contact with low-phosphate media reprograms plant root architecture. Nat Genet 39: 792-796

Pubmed: [Author and Title](#)

CrossRef: [Author and Title](#)

Google Scholar: [Author Only](#) [Title Only](#) [Author and Title](#)

van der Maaten L (2013) Barnes-Hut-SNE. arXiv:1301.3342[cs.LG]

Pubmed: [Author and Title](#)

CrossRef: [Author and Title](#)

Google Scholar: [Author Only](#) [Title Only](#) [Author and Title](#)

van der Maaten L, Hinton G (2008) Visualizing Data using t-SNE. Journal of Machine Learning Research 9: 2579-2605

Pubmed: [Author and Title](#)

CrossRef: [Author and Title](#)

Google Scholar: [Author Only](#) [Title Only](#) [Author and Title](#)

Wang J, Tian L, Lee HS, Wei NE, Jiang H, Watson B, Madlung A, Osborn TC, Doerge RW, Comai L, Chen ZJ (2006) Genomewide nonadditive gene regulation in Arabidopsis allotetraploids. Genetics 172: 507-517

Pubmed: [Author and Title](#)

CrossRef: [Author and Title](#)

Google Scholar: [Author Only](#) [Title Only](#) [Author and Title](#)

Werner JD, Borevitz JO, Warthmann N, Trainer GT, Ecker JR, Chory J, Weigel D (2005) Quantitative trait locus mapping and DNA array hybridization identify an FLM deletion as a cause for natural flowering-time variation. Proc Natl Acad Sci U S A 102: 2460-2465

Pubmed: [Author and Title](#)

CrossRef: [Author and Title](#)

Google Scholar: [Author Only](#) [Title Only](#) [Author and Title](#)

West MA, Kim K, Kliebenstein DJ, van Leeuwen H, Michelmore RW, Doerge RW, St Clair DA (2007) Global eQTL mapping reveals the complex genetic architecture of transcript-level variation in Arabidopsis. Genetics 175: 1441-1450

Pubmed: [Author and Title](#)

CrossRef: [Author and Title](#)

Google Scholar: [Author Only](#) [Title Only](#) [Author and Title](#)

Wickham H (2009) ggplot2: elegant graphics for data analysis. Springer New York

Pubmed: [Author and Title](#)

CrossRef: [Author and Title](#)

Google Scholar: [Author Only](#) [Title Only](#) [Author and Title](#)

Xu F, Guo W, Xu W, Wei Y, Wang R (2009) Leaf morphology correlates with water and light availability: What consequences for simple and compound leaves?. Progress in Natural Science 19(12): 1789-1798

Pubmed: [Author and Title](#)

CrossRef: [Author and Title](#)

Google Scholar: [Author Only](#) [Title Only](#) [Author and Title](#)

Xu K, Xu X, Fukao T, Gantier P, Ming F, Wang R, Rodriguez R, Houde S, Small AM, Bailey-Serres J, Ronald FC, Mackill DJ (2006) Sub1A is an ethylene-response-factor-like gene that confers submergence tolerance to rice. Nature 442: 705-708

Pubmed: [Author and Title](#)

CrossRef: [Author and Title](#)

Google Scholar: [Author Only](#) [Title Only](#) [Author and Title](#)

Young MD, Wakefield MJ, Smyth GK, Oshlack A (2010) Gene ontology analysis for RNA-seq: accounting for selection bias. Genome Biol 11: R14

Pubmed: [Author and Title](#)

CrossRef: [Author and Title](#)

Google Scholar: [Author Only](#) [Title Only](#) [Author and Title](#)

Yu D, Chen C, Chen Z (2001) Evidence for an important role of WRKY DNA binding proteins in the regulation of NPR1 gene expression. Plant Cell 13: 1527-1540

Pubmed: [Author and Title](#)

CrossRef: [Author and Title](#)

Google Scholar: [Author Only](#) [Title Only](#) [Author and Title](#)

Zhang L, Fetch T, Nirmala J, Schmierer D, Brueggeman R, Steffenson B, Kleinhofs A (2006) Rpr1, a gene required for Rpg1-dependent resistance to stem rust in barley. Theor Appl Genet 113: 847-855

Pubmed: [Author and Title](#)

CrossRef: [Author and Title](#)

Google Scholar: [Author Only](#) [Title Only](#) [Author and Title](#)

Zhang X, Cal AJ, Borevitz JO (2011) Genetic architecture of regulatory variation in Arabidopsis thaliana. Genome Res 21: 725-733

Pubmed: [Author and Title](#)

CrossRef: [Author and Title](#)

Google Scholar: [Author Only](#) [Title Only](#) [Author and Title](#)